

A Systematic Performance Analysis of Deep Perceptual Loss Networks Breaks Transfer Learning Conventions

Gustav Grund Pihlgren*, Konstantina Nikolaidou*, Prakash Chandra Chhipa*, Nosheen Abid*,
Rajkumar Saini*, Fredrik Sandin*, Marcus Liwicki*

*Machine Learning Group
Luleå University of Technology, Sweden
{firstname}.{lastname}@ltu.se

Abstract—Deep perceptual loss is a type of loss function in computer vision that aims to mimic human perception by using the deep features extracted from neural networks. In recent years the method has been applied to great effect on a host of interesting computer vision tasks, especially for tasks with image or image-like outputs, such as image synthesis, segmentation, depth prediction, and more. Many applications of the method use pretrained networks, often convolutional networks, for loss calculation. Despite the increased interest and broader use, more effort is needed toward exploring which networks to use for calculating deep perceptual loss and from which layers to extract the features.

This work aims to rectify this by systematically evaluating a host of commonly used and readily available, pretrained networks for a number of different feature extraction points on four existing use cases of deep perceptual loss. The four use cases are implementations of previous works where the selected networks and extraction points are evaluated instead of the networks and extraction points used in the original work. The experimental tasks are dimensionality reduction, image segmentation, super-resolution, and perceptual similarity. The performance on these four tasks, attributes of the networks, and extraction points are then used as a basis for an in-depth analysis. This analysis uncovers essential information regarding which architectures provide superior performance for deep perceptual loss and how to choose an appropriate extraction point for a particular task and dataset. Furthermore, the work discusses the implications of the results for deep perceptual loss and the broader field of transfer learning. The results break commonly held assumptions in transfer learning, which imply that deep perceptual loss deviates from most transfer learning settings or that these assumptions need a thorough re-evaluation.

I. INTRODUCTION

In the last decade, machine learning for computer vision has evolved significantly. This evolution is mainly due to the developments in artificial neural networks. An essential focus of these developments has been the calculation of the loss used to train models. Several methods build on using neural networks to calculate the loss for another machine learning model. Among these methods are milestone achievements such as adversarial examples [1], generative adversarial networks [2], deep visualization [3], and saliency maps [4]. In this work, the practice of training a model by feeding its output into a deep neural network and using outputs or deep features (activations)

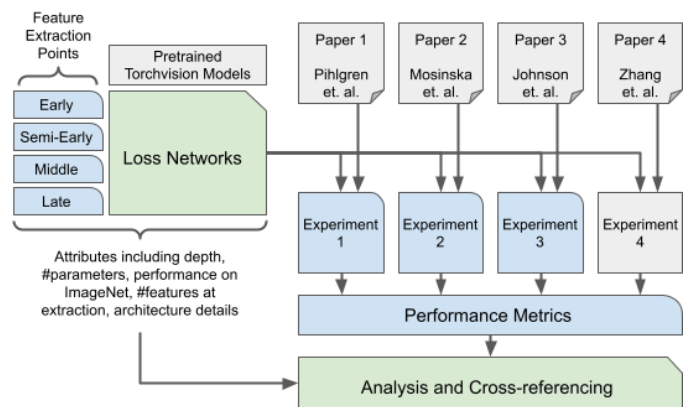


Fig. 1. The contribution of this work is a deep investigation into the influence of different attributes of loss networks, building on the existing procedures of four baseline papers. A systematic evaluation of loss networks created with pretrained networks from 14 different architectures with four different extraction points is performed to gain new insights regarding the use of deep perceptual loss. The areas where this work makes some contribution are in blue (rounder-corner) and the primary novelties are in green (cut-corner).

from that network to calculate the loss will be referred to as deep feature loss and the network used in loss calculation is referred to as the loss network.

Two methods that have extensively used deep feature loss are perceptual losses and similarity metrics. The goal of similarity metrics is to create a function $f(x_0, x_1)$ that computes the similarity or distance between the two data points x_0 and x_1 in some domain. In the domain of computer vision, similarity metrics are often used to compare the similarity of two images. The related field of perceptual loss aims to create loss functions for machine learning models that mimic human perception. Such a loss function is referred to as a perceptual loss and is often inspired by human perception. Perceptual loss is mainly used to estimate human perception of quality and similarity. In the latter case, a perceptual loss is also a similarity metric. A perceptual loss that uses deep features is referred to as a deep perceptual loss, which is what is being explored in this work.

Deep perceptual loss has been a natural progression of deep feature loss for image synthesis, where it is utilized to improve

performance on various tasks. These tasks include style-transfer [5], image generation [6], super-resolution [7], image denoising [8], and more. In addition to image synthesis, the method has been successful for tasks with image-like outputs such as image segmentation [9], dimensionality reduction [10], and image depth prediction [11]. Additionally, comparing deep features has become the dominant technique for measuring the perceptual similarity of images [12]. With the widespread use of deep perceptual loss, a study into how to utilize the method is well justified, which is the purpose of this work.

A. Purpose of the study

This work aims to give insight into how to select pretrained loss networks and from which layers to perform feature extraction to get the most useful deep perceptual loss for a task. Prior works that used loss networks typically justified their choice of network, if at all, by performance on another task or prior use. Additionally, the choice of extraction point is rarely justified at all. This work aims to take a more systematic approach and test a wide variety of easily accessible and well-known pretrained Convolutional Neural Networks (CNNs) architectures and compare their performance as loss networks for four different extraction points. Their performance is evaluated on four prior works that have used pretrained loss networks. The experiments of those previous works have been repeated using many different loss networks that were not tested originally. These four previous works are referred to as the baseline papers. The results obtained from these experiments have been analyzed to gain insight into how the choice of architecture and feature extraction point affects performance. These insights have been the basis for further suggestions on how to select pretrained architectures and extraction points for loss networks. An illustration of the procedure followed in this work, from the baseline papers and loss networks to the analysis, is shown in Fig 1.

B. Scope

For a deep perceptual loss function, an abundance of neural network architectures are available, plenty of datasets that could be used to train them, and a plethora of ways to perform feature extractions from those networks. It is clearly outside the scope of any one study to look into them all.

This work explores the pretrained models for some of the classification architectures provided by Torchvision [13], a package of the PyTorch [14] framework. All of the selected models have been pretrained with the ImageNet [15] dataset. These networks, with or without pretrained parameters, are readily available for public use, which is itself a motivation for their usage; however, there are more reasons for using the networks provided in Torchvision. The pretrained neural networks available in Torchvision contain a wide variety of architectures based on several renowned papers. There are also multiple different implementations of the different networks within Torchvision. This provides the ability to test how different architectures behave as loss networks and how this behavior changes with more minor changes in implementation. Additionally, applications of deep perceptual loss commonly

use the pretrained networks in Torchvision to create loss networks.

Another limitation in scope is that only models pretrained on ImageNet are used in the loss networks. While exploring how different pretraining procedures and datasets affects the loss networks is an interesting proposition, this is left for future works to investigate. Aside from ease of access, the ImageNet dataset is a good choice for loss network pretraining as it is one of the largest and most well-used computer vision datasets.

This work also investigates how the choice of the layers in the loss networks that feature extractions is made from affects the trained models. In this work, the loss networks extract features in a straightforward manner. For a given architecture and extraction point, the activations are propagated forward to the extraction point and then used directly to calculate the loss. While more elaborate feature extraction methods exist, they are not considered in this work.

C. Contributions

The contributions of this work are as follows:

- A systematic evaluation and analysis of the performance of a variety of CNN architectures and extraction points when they are used as loss networks for deep perceptual loss and similarity.
- Supplementary material containing the results of the evaluation for further analysis (more details in the Appendix).
- An in-depth analysis as to which architecture and extraction points to use for loss networks, for a given task and dataset.
- A discussion regarding some interesting correlations and lack thereof and their implication for the field.
- Suggestions for future work based on those interesting findings, especially that some longstanding transfer learning conventions in the computer vision domain are in need of re-evaluation.

II. BACKGROUND

The terminology of the subfield of perceptual loss is not always used consistently between pieces of literature. For clarity, this section is prefaced with a description of how some common terms are used in this work. Additionally, these terms are introduced with greater detail throughout the literature review.

- A perceptual loss is a loss function that is meant to estimate some factor of human perception, often with the goal of having model predictions be closer to those of humans.
- A loss network is a neural network that is used as part of the loss calculation for the training of another machine learning model. Though for cohesion this work also uses the term loss network to refer to networks used to extract image similarity.
- Deep feature loss is when the output of a machine learning model is fed into a loss network and deep features extracted from that loss network are used for the loss calculation of the original model.
- Deep perceptual loss is when deep feature loss is used to create a perceptual loss.

A. Feature Extraction

Feature extraction in machine learning is the process of converting input data into descriptive and non-redundant features. Before feature learning became widely adopted, most feature extraction used methods handcrafted by experts to find the appropriate attributes in the data that were good enough. This type of feature extraction can drastically reduce dimensionality but demands expert knowledge [16]. Further, successful algorithms for feature extraction and their applications were introduced and can be found in the literature, such as restricted Boltzmann machines [17], sparse-coding [18], and K-means [19]. These methods have used simple low-level features such as "blobs" and "edges". With the advancement of the deep models and autoencoders [20, 21] feature extraction has been automated to cater to complex invariances in the data [19]. Feature extraction using deep models has been successfully used in many applications [16, 22, 23, 24, 25]

Which architecture to use for feature extraction and how to pretrain them is a difficult question to answer, where the best practices often vary between fields and even between individual tasks. For example, it's been shown that for unsupervised pretraining one cannot necessarily assume that better pretraining performance leads to better downstream performance [26]. However, for many computer vision tasks, the trend has been that using pretrained models that perform better on ImageNet [15] lead to better downstream performance [27].

B. Pixel-wise loss

A wide variety of machine learning models use loss calculation as part of the learning process, where the goal of training is to minimize the loss (or in equivalent cases maximize the reward). Many different factors can be considered when defining the loss for a certain training procedure. So-called regulatory losses can be used to enforce certain properties, by increasing the loss with increasing deviation from those properties. Extrinsic rewards from some environments can directly be used as a loss. However, usually, when loss calculation is considered in machine learning it involves comparing the model output with some desired output. This is sometimes called error, as in the error made in estimating the desired output. As a lot of the current state-of-the-art of machine learning is trained to estimate some desired output, how to calculate the difference is of great interest.

A loss function that calculates the difference between a model's output and the desired output is by definition also a similarity metric for the output domain. When the output is an image any loss function used could then be viewed as calculating the similarity between two images, which is an open and arguably unsolvable problem. Previously, machine learning models with image and image-like outputs have been trained with loss based on pixel-wise metrics. Pixel-wise metrics work by aggregating the differences between the corresponding pixels in the two images. However, pixel-wise metrics are widely known to be flawed measurements of similarity, especially when estimating human perception [6].

C. Deep Feature and Deep Perceptual Loss

A method for computing the loss of a machine learning model that has grown in popularity alongside deep learning is deep feature loss. Deep feature loss is when a part of the loss calculation is made by using the features of a deep neural network other than the one being trained by the loss. In such a use case the neural network used to generate the loss is referred to as a loss network.

While deep feature loss is often considered to require the use of a deep neural network, the practice of using features from one neural network to generate the loss for another has been around for longer than deep learning. For example, predictability minimization, which was published in 1992, trains a perceptron to do encoding by using a loss generated by another perceptron when given the encoding as input [28]. Deep feature loss using deep learning though, was introduced in the field of explainable AI to optimize the input image for certain classes [29] and later individual neurons [3]. Soon after it was used for adversarial training for adversarial examples [1] and Generative Adversarial Networks [2]. These works were soon followed by a host of uses of deep feature loss.

In this work, when deep feature loss is used as part of a perceptual loss this is referred to as a deep perceptual loss. The naming convention is used to differentiate from other methods that are described as perceptual loss that do not use deep features. Deep perceptual loss was first used with neural style transfer [5] where features from a pretrained version of VGG-19 [29] were used to estimate perceptions of style and content. These perceptions were then used as a loss to generate images with the perceived content of one image and the perceived style of another.

Since this introduction deep perceptual loss has been a popular tool for image generation tasks. It was used in the VAE-GAN in which the discriminator acts as a loss network to facilitate higher quality image generation [6]. In the VAE-GAN the discriminator is trained alongside the generator, but other works have used pretrained loss networks instead removing the need for extra training [30].

Other popular uses tend to be adjacent to the image generation domain, where the output of the model is a 2-dimensional lattice such as image segmentation [31], feature heat maps for object detection [32], and depth prediction [11]. This is not so surprising as deep perceptual loss was first developed in the computer vision domain and tends to use models pretrained on images as loss networks. As such, the deep features of these networks are more useful when extracted from images and image-like inputs.

However, not all models that output 2-dimensional lattices during training are used for that purpose. Convolutional autoencoders, for example, are often used for dimensionality reduction instead of image generation. Deep perceptual loss has been proven effective in this case as well [10].

D. Perceptual Similarity Metrics

A closely related field to perceptual loss is perceptual similarity. The goal of perceptual similarity is to find metrics that estimate the human perception of visual similarity. As the

point of loss functions is typically to identify the difference between the target and the output of a model, a perceptual similarity metric could be used directly as a loss function. For example, the Structural Similarity Index Measure (SSIM) [33] was introduced as a perceptual similarity metric and then later used a perceptual loss function [34, 35].

With deep perceptual loss, the procedure was the inverse, as the methods for calculating deep perceptual loss developed first and were later adapted as a metric for perceptual similarity [12]. Since this use is no longer a loss function, the method of using deep features to calculate perceptual similarity is referred to as deep perceptual similarity.

Deep perceptual similarity metrics, like deep perceptual loss, most commonly make use of pretrained networks. Training the networks specifically for perceptual similarity can give a small increase in performance [12], especially when used together with ensemble methods [36]. However, this improvement is marginal at best, which attests to how effective pretrained CNN features are for perceptual similarity.

A recent study has analyzed how different network architectures and pretraining methods affect performance on deep perceptual similarity [27]. This recent study shares similarities in methodology to this work, however, it did not examine deep perceptual loss, which is the main purpose of this work. The results from this recent study show that better pretraining performance does not directly lead to a better perceptual similarity metric. In fact, after a certain point better pretraining performance is shown to be detrimental to performance on perceptual similarity. The upper bound for perceptual similarity performance as a function of ImageNet accuracy is shown to steadily increase until a threshold, after which it decreases. While prior studies have also shown a lack of correlation between pretraining performance and downstream performance [26], the clear increase of performance to a certain point followed by a clear decrease is surprising. It is additionally shown that the model and pretraining have a huge impact on perceptual similarity. For this purpose selecting the right architecture and pretraining procedure is more important than any training on actual perceptual similarity data.

E. Applications

Deep perceptual loss is frequently used in image synthesis tasks like image fusion [37], style-transfer [7], and super-resolution [38]. Deep perceptual loss has also been adapted for better results in many domains like medical images [8] and earth observation [39]. In addition to analyzing deep perceptual similarity, this work focuses on three applications of deep perceptual loss.

The first application considered in this work is dimensionality reduction of images through autoencoding for downstream tasks. Here deep perceptual loss is used to calculate the similarity of the reconstructed image to the original as part of the so-called reconstruction loss. The second application is delineation of images, which is a form of image segmentation, for which deep perceptual loss is used to calculate the difference between the output segmentation to the desired one. The third application is super-resolution, where deep perceptual loss is used to compare the up-scaled output image with the known full-scale image.

1) *Autoencoding*: Autoencoders have been used for decades as a tool for dimensionality reduction and feature learning [40, 41]. They have also been used for purposes beyond dimensionality reduction, such as image generation [42]. In the last couple of years, deep perceptual loss has been used to train autoencoders for image generation [6] and more recently also for their original dimensionality reduction purposes [10].

2) *Image segmentation*: Image segmentation is the task of, at the pixel level, dividing an image into different segments representing classes or instances. Since each pixel of the image is assigned a class or instance, the output of a segmentation model is a 2-d lattice. This 2d-lattice can be interpreted as an image and deep perceptual loss can be used to compare the output segmentation with the desired segmentation. Using deep perceptual loss to train segmentation models is has been used in applications such as delineating roads in aerial images, locating cracks in roads, and finding edges of cells in microscopy [31]. Additionally, deep perceptual loss has been used in the segmentation of medical images [9].

3) *Super-resolution*: Super-resolution is the task of transforming a low-resolution image into a high-resolution image. The usefulness of models with this capability can be found in real-world applications such as security and medical image processing or within other algorithms to enhance the performance of different computer vision tasks [43]. Like with image segmentation, deep perceptual loss has become widely adopted for training super-resolution models [7, 44], including for important medical applications [8].

F. Pretrained Torchvision networks

The Torchvision package [13] provides many different renowned CNN architectures that at some point have been state-of-the-art for image processing. This section briefly covers the accomplishments, innovations, and general design of the architectures found in Torchvision that are used in this work. However, this section does not go into implementation details for each of the networks. For such information, the reader is referred to the papers that introduced those architectures. Details for how Torchvision's pretrained models for each architecture perform on the ImageNet top-1 and top-5 classification accuracy tasks can be found in Table I.

1) *AlexNet*: AlexNet is the name given to the network introduced by Krizhevsky et al. [54] and further built upon in [51]. A variant of the network won the ILSVRC-2012 [15] competition, marking the first time a neural network won the challenge and is often seen as one of the starting points of the current wave of deep learning.

AlexNet follows what is considered a basic CNN architecture with 5 convolutional layers followed by 3 fully-connected layers. The first convolutional layer has a kernel size of 11 and stride 4 which is large compared to most recent networks. While AlexNet has lower performance and robustness than more recent CNN architectures [55], its features have proven competitive to those same networks when used as a perceptual similarity metric [12].

2) *VGG*: VGG is an innovative object-detection deep model proposed by Simonyan and Zisserman in 2012 [45]. It is a

TABLE I
PERFORMANCE OF PRETRAINED TORCHVISION MODELS ON IMAGENET.

Architecture	Top-1 Acc.	Top-5 Acc.
<i>VGG Networks</i>		
VGG-11 [45]	69.020	88.628
VGG-16 [45]	71.592	90.382
VGG-16_bn [45]	73.360	91.516
VGG-19 [45]	72.376	90.876
<i>Residual Networks</i>		
ResNet-18 [46]	69.758	89.078
ResNet-50 [46]	76.130	92.862
ResNeXt-50 32x4d [47]	77.618	93.698
<i>Inception Networks</i>		
GoogLeNet [48]	69.778	89.530
InceptionNet v3 [49]	77.294	93.450
<i>EfficientNet</i>		
EfficientNet_B0 [50]	77.692	93.532
EfficientNet_B7 [50]	78.642	94.186
<i>Uncategorized Networks</i>		
AlexNet [51]	56.522	79.066
DenseNet-121 [52]	74.434	91.972
SqueezeNet 1.1 [53]	58.178	80.624

CNN that outperformed conventional deep models and is one of the best object-detection models even today.

As compared to AlexNet, VGG has an essential factor of depth. VGG has a smaller kernel size of 3 with a stride of 1, which is common for more recent CNNs. It also uses 1×1 convolution to incorporate more non-linearity in the decision function without changing the receptive fields. VGG uses small-size convolution filters that allow the integration of more weighted layers. VGG variants have won first and second place in the ILSVRC-2014 competition. This paper explores some of its versions, namely, VGG-11, VGG-16, VGG-19, and a version of VGG-16 that uses batch-normalization called VGG-16_bn.

3) *Residual Networks*: After AlexNet won ILSVRC-2012, every subsequent winning architecture increased the number of layers. However, increasing the number of layers without additional changes can lead to the common issues of vanishing and exploding gradients. To solve the problem of vanishing or exploding gradients, residual networks (ResNet) using skip connections were introduced [46]. Skip connections connect later layers to earlier ones skipping a few layers in between. There are many updated versions of ResNet introduced later to improve the performance. One of the subsequent versions, called ResNeXt-50, redesigned the fundamental building block of ResNet to use a multi-branch setup similar to inception networks [47].

This paper has worked with three types of residual networks, namely, ResNet-18, ResNet-50, and ResNeXt-50 32x4d.

4) *SqueezeNet*: While much of the contemporary research on deep CNNs focused on improving the performance, Iandola et al. [53] focused on reducing the size of deep models by proposing SqueezeNet. It has a similar performance to

AlexNet with 50 times fewer parameters. Smaller models, like SqueezeNet, can fit on smaller servers, require less communication for distributed training, can easily be exported to edge servers and products, and are also suitable to deploy on more limited hardware such as FPGAs. To achieve these benefits, SqueezeNet has reduced the kernels with size 3 to 1×1 convolutions, use squeeze layers to decrease the number of input channels to the kernels, and downsample later in the architecture to have large activation maps with the assumption that it leads to higher classification accuracy.

5) *Inception Networks*: Inception Network [48] was a remarkable breakthrough in the field of computer vision introduced in 2015. So far, the deep learning models were getting deeper and deeper with the assumption that the deeper the model, the better the learning. Very deep networks are prone to overfitting, and passing the gradient updates through the entire network becomes challenging. Considering the variations in the information location, choosing the appropriate filter size became difficult. If the filter size is large, it may lose the distribution locally, and if the filter is small, it may lose the information distributed globally. To deal with these challenges, Inception Network came up with the concept of multiple size filters at each layer, leading the network to be "wider" rather than "deeper". Inception networks became a new state-of-the-art architecture for classification and detection in the ILSVRC. Multiple networks building on the basic inception network template have been introduced with improved performance. This paper has explored the first version of Inception Network developed by the Google team, *i.e.*, GoogLeNet [48] and Inception Network version 3 [49].

6) *DenseNet*: DenseNet [52] got the best paper award in CVPR 2017. It focused on using fewer parameters with densely connected layers to achieve higher accuracy. It is composed of dense blocks. Each layer in the dense block takes the feature maps of preceding layers as input. This concept of DenseNet reduces the vanishing gradient problem, improves feature propagation, stimulates feature reuse, and considerably reduces the number of parameters. In this work, the DenseNet-121 implementation is examined.

7) *EfficientNet*: EfficientNet [50] is a recent release of 2020. It is a CNN-based architecture that uses compound coefficients to uniformly scale the architecture's dimensions. Unlike traditional methods that arbitrarily scale these factors, EfficientNet uses a set of fixed scaling coefficients to scale the network in a principled way uniformly. The authors stated that its 8.4 times smaller and 6.1 times faster on inference than existing state-of-the-art CNN models. In this paper, two versions of EfficientNet are used corresponding to the ones with the fewest and most layers, *i.e.*, EfficientNet_B0 and EfficientNet_B7.

III. THE BASELINE PAPERS

In order to evaluate the effects of different pretrained loss network architectures and feature extraction points this work recreates the experiments of four papers that are relevant to the field. These experiments are extended by testing loss networks using additional architectures and extraction points to observe

how the results vary. These observations are then used as a starting point for an in-depth analysis of what attributes make a good loss network.

Rather than designing experiments for this purpose, which might risk abstracting away the concrete uses of pretrained loss networks, this work implements the experiments of four prior works in the field which cover different uses of the method. These works are referred to as the baseline works and are assigned numbers for easy reference. The baseline works are *Pretraining Image Encoders without Reconstruction via Feature Prediction Loss* [56] (Paper 1), *Beyond the Pixel-Wise Loss for Topology-Aware Delineation* [31] (Paper 2), *Perceptual Losses for Real-Time Style Transfer and Super-Resolution* [7] (Paper 3), and *The Unreasonable Effectiveness of Deep Features as a Perceptual Metric* [12] (Paper 4).

A. Pretraining Image Encoders without Reconstruction via Feature Prediction Loss

In Paper 1, an AlexNet model pretrained on ImageNet with feature extraction after the 2nd ReLU is used as a loss network to train autoencoders to encode features for downstream predictions. The autoencoders trained with deep perceptual loss are then compared to those trained with pixel-wise loss as well as those trained using a proposed feature prediction loss. To perform the comparison the autoencoders are used as feature extractors for MLP models trained on downstream tasks on the datasets STL-10 [57], SVHN [58], and LunarLander-v2 [59] collection. The results show that deep perceptual loss and feature prediction loss both significantly outperforms pixel-wise loss on the downstream tasks and that of those two feature prediction loss takes only around 2/3 of the computation time to train.

Paper 1 evaluates the use of pretrained networks for deep perceptual loss as well as feature prediction loss for the use of training autoencoders for downstream prediction. While deep perceptual loss has been used to train autoencoders in many other works, this has often not been for the purpose of feature extraction for downstream prediction. It also introduces feature prediction loss, which is not technically a deep perceptual loss, but with similarities that warrants exploring.

The experiments in Paper 1 use convolutional encoders and decoders for images and single hidden layer MLPs for encoding and decoding features. The details of the encoders and decoders can be found in Table II. Where z denotes the encoding size (64, 128, or 256), *UNK* means that the size has to be calculated based on image size and loss network and stride is 2 for all convolutional and deconvolutional layers.

The paper evaluates autoencoders using standard image encoding and decoding, as well as replacing the image encoding with feature extraction and replacing image decoding with directly predicting the features of a loss network. The latter is dubbed, feature prediction loss. To do this the paper evaluates all combinations of the encoder and decoders presented with pixel-wise, deep perceptual, and feature prediction loss. The three losses are presented in Eq. 1-3 respectively, where en stands for encoder, de for decoder, ϕ a loss network with m features, and f a loss function. In the paper, AlexNet is used as

TABLE II
ENCODER AND DECODER USED IN PAPER 1

Layer	#Kernels	Kernel size	Size
<i>Image Encoder</i>			
Conv2d - BatchNorm - ReLU	32	4	-
Conv2d - BatchNorm - ReLU	64	4	-
Conv2d - BatchNorm - ReLU	128	4	-
Conv2d - BatchNorm - ReLU	256	4	-
Fully Connected	-	-	z
<i>Feature Encoder</i>			
Fully Connected	-	-	2048
Fully Connected	-	-	z
<i>Image Decoder</i>			
Fully Connected	-	-	<i>UNK</i>
Deconv2d - BatchNorm - ReLU	128	5	-
Deconv2d - BatchNorm - ReLU	64	5	-
Deconv2d - BatchNorm - ReLU	32	6	-
Deconv2d - BatchNorm - ReLU	3	6	-
<i>Feature Decoder</i>			
Fully Connected	-	-	2048
Fully Connected	-	-	<i>UNK</i>

a loss network with features extracted after the second ReLU, and Mean-Square error is used as the loss function.

$$L_{pw}(x) = \sum_{k=1}^n f(x_k, de(en(x))_k) \quad (1)$$

$$L_{dp}(x) = \sum_{k=1}^m f(\phi(x)_k, \phi(de(en(x)))_k) \quad (2)$$

$$L_{fp}(x) = \sum_{k=1}^m f(\phi(x)_k, de(en(x))_k) \quad (3)$$

Each autoencoder setup is then trained for 50 epochs without labels on one portion of the dataset. The trained autoencoders are then used to encode the labeled parts of the datasets. Then multiple MLPs with no, one, or two hidden layers are trained for 500 epochs using the encoded data to perform the task associated with the dataset. For each autoencoder, the MLP with the best performance on the validation set is evaluated on the test set. The performance of an autoencoder is then equated to the performance of its downstream MLP as a high-performing MLP is indicative of good encoding.

These experiments are repeated four times and the average test scores are reported.

B. Beyond the Pixel-Wise Loss for Topology-Aware Delineation

Paper 2 focuses on the problem of delineating curvilinear structures through semantic segmentation tasks, specifically focusing on the inability of pixel-wise losses to consider topological details. The paper proposes a topology-aware loss to complement the pixel-wise binary cross entropy (BCE) loss based on the feature maps of the first, second, and third layers of the VGG-19 network pretrained on ImageNet. It uses U-Net [60] as the primary trainable model for the above-explained

downstream task. Topology loss minimizes the differences between the VGG-19 descriptors of the ground-truth images and the corresponding predicted delineations shown in Eq. 4

$$L_{top}(x, y) = \sum_{n=1}^N \frac{1}{C_n H_n W_n} \sum_{m=1}^{C_n} \|\phi_n^m(y) - \phi_n^m(U(x))\|_2^2 \quad (4)$$

where x and y are the input image and ground truth lattice of labeled pixels, U is the U-net model being trained, ϕ_n^m is m -th feature map in the n -th layer of the VGG-19 network, N is the number of convolutional layers and C_n is the number of channels in the n -th layer, each of size $W_n \times H_n$. L_{top} measures the difference between the higher-level visual features of the linear structures in the ground truth and those in the predicted image. L_{top} is combined with BCE loss with scalar weighing. Further improvements in predictions are proposed using iterative refinement to eliminate the mistakes, e.g., small gaps in lines. Paper 2 compares the performance of using deep perceptual loss with BCE loss and Reg-AC [61]. The results are compared using the completeness, correctness, and quality of delineation as introduced in [62]. In short, completeness, correctness, and quality are analogues to recall, precision, and critical success index respectively. The method is evaluated on three datasets of different linear structures, Cracks [63], The Massachusetts Roads Dataset [64], and Electron Microscopy images from the ISBI'12 challenge [65]. Results indicate that combining topology loss and iterative refinement with pixel-wise loss improves the quality of predicted delineations.

C. Perceptual Losses for Real-Time Style Transfer and Super-Resolution

Paper 3 uses deep perceptual loss for two image transformation tasks, style transfer and single-image super-resolution. A VGG-16 model pretrained on ImageNet with features extracted at various points is used as the loss network. The paper compares the use of perceptual loss with the work presented in [66] for style transfer and the work presented in [67] for super-resolution. Qualitative and speed results are presented for style transfer and suggest that the use of perceptual loss can conclude in similar results as the compared works but with increased speed. For super-resolution, Paper 3 performs the task for a factor of $\times 4$ and $\times 8$ and evaluates on the datasets Set5 [68], Set14 [69], and BSD100 [70] using PSNR and SSIM metrics.

For the super-resolution experiments, Paper 3 uses a residual network as a transformation network which takes as input a blur version of the ground truth and tries to reconstruct a super-resolution image that minimizes a feature reconstruction loss formalized in Eq. 5. This loss enforces the input x and output \hat{x} images to be close by computing the Euclidean distance between the feature representations of the n th layer $\phi_j(x)$ and $\phi_j(\hat{x})$, where ϕ represents the loss network.

$$L_{feat}^{\phi, n}(\hat{x}, x) = \frac{1}{C_n H_n W_n} \|\phi_n(\hat{x}) - \phi_n(x)\|_2^2 \quad (5)$$

D. The Unreasonable Effectiveness of Deep Features as a Perceptual Metric

Paper 4 concerns the use of deep features of pretrained CNNs as a similarity metric for images. It introduces the BAPPS dataset and uses it to train and evaluate a number of different models based on both pretrained and randomly initialized CNNs. The findings of the paper show that on the BAPPS dataset deep perceptual similarity metrics outperform prior rule-based methods when it comes to mimicking human perception of similarity.

While Paper 4 does not fall under the label deep perceptual loss as the neural networks are not used to generate the loss for any other model, the use of CNNs as similarity metrics is the same as when that similarity score is used as a deep perceptual loss in other works. This together with the direct comparison of how well deep features actually mimic human perception of similarity are the reasons for the selection of this paper as one of the baselines, despite not technically using deep perceptual loss. For the sake of cohesion, the networks used in Paper 4 to create the similarity metrics will be referred to as loss networks regardless.

The implementation presented in Paper 4 follows the same general procedure as most uses of loss networks to measure similarity. The metric used to calculate the similarity of x and x_0 is described in Eq. 6, where z and z_0 are the channel-wise unit-normalized feature extractions from the loss network and w are the importance weights.

$$d(x, x_0) = \sum_n \frac{1}{H_n W_n} w_n \odot \|z_n - z_{0n}\|_2^2 \quad (6)$$

Paper 4 evaluates many different neural network models as loss networks. All of the evaluated models use variants of AlexNet as their architecture with varying approaches for setting the parameters of the network. The approaches are random initialization, k-means initialization [71], self-supervision using video [72], self-supervision using split-brain autoencoding [73], self-supervision using puzzle-solving [74], generative modelling [75], pretrained networks, pretrained networks with importance weights optimized using BAPPS, pretrained networks fine-tuned using BAPPS, and networks trained from scratch using BAPPS. The last four approaches all use the Torchvision versions of VGG16 and SqueezeNet in addition to the Torchvision version of AlexNet.

IV. DATASETS

This work extends the experiments of four existing works. As such it makes use of some of the datasets used in those works which are described in this section. How the datasets are used is further described in the Experimental Details section. The datasets used in this work and their associated works are STL-10 [57] and Street View House Numbers (SVHN) [58] in Paper 1, Massachusetts Roads Dataset (MRD) [64] in Paper 2, MSCOCO [76], Set5 [68], Set14 [69] and BSD100 [70] in Paper 3, and Berkeley Adobe Perceptual Patch Similarity (BAPPS) [12] in Paper 4.

A. STL-10

STL-10 is an image dataset consisting of 108500 photos of animals and vehicles. The photos are a subset of the larger ImageNet [15] dataset that has been scaled to 96×96 pixels. The dataset is divided into three parts, 500 labeled training images, 8000 labeled testing images, and 100000 unlabeled images. The labeled images are split among 10 classes of animals and vehicles while the unlabeled data contains images both from the 10 classes as well as from other animals and vehicles. The intent is to use the unlabeled data to design or learn priors that can help improve models trained on the training images. The dataset is prominently used for unsupervised and self-supervised feature learning.

STL-10 comes with a predefined 10-fold training and testing protocol, however, this protocol is not used in this work as it was not used by the work that is being recreated. This means that the results from this work cannot be directly compared to prior uses of the dataset that followed the protocol.

B. SVHN

SVHN is an image dataset consisting of photos of house numbers where the individual digits have been given bounding boxes and labeled. The dataset is available with both the original photos as well as the individual digits cropped out and scaled to 32×32 pixels. The individual digits are split into three parts, 73257 for training, 26032 for testing, and 531131 extra for various purposes.

In this work, the extra images are used for unlabeled pretraining.

C. MRD

MRD is an image dataset consisting of 1171 aerial images covering roads and streets in various terrains. The images are 1500×1500 pixels, where each pixel corresponds to a square meter of surface area. For each image, there is a target segmentation map, where each pixel is labeled as either road or background. The dataset is split into a training set of 1108 images, a validation set of 14 images, and a test set of 49 images.

D. MSCOCO - Set5 - Set14 - BSD100

Train - Validation: MS COCO (Common Objects in Context) is a large-scale dataset of natural images used for object detection, dense pose estimation, keypoint detection, image captioning, and semantic, instance, and panoptic segmentation. The dataset includes 200K labeled and 130K unlabeled images that have been used for several years in the COCO Challenge, one of the most popular competitions for computer vision tasks. In this work, only a subset of the train images is used without the use of any labels for the task of super-resolution, where the original high-resolution (HR) images are used as ground truth and a blur version of them as input.

Test: Set5, Set14, and BSD100 are the standard test sets used for the evaluation of super-resolution methods. The datasets consist of 5, 14, and 100 RGB images of different sizes, respectively, depicting animals and humans.

TABLE III
BAPPS DATA SPLITS

Split	Distortion	Samples
2AFC Train	Traditional	56.6k
	CNN-based	38.1k
	Mixed	56.6k
	Total	151.4k
2AFC Test	Traditional	4.7k
	CNN-based	4.7k
	Superres	10.9k
	Frame Interp	1.9k
	Video Deblur	9.4k
	Colorization	4.7k
	Total	36.3k
JND Test	Traditional	4.8k
	CNN-based	4.8k
	Total	9.6k

E. BAPPS

BAPPS is an image dataset consisting of 64×64 image patches sampled from the MIT-Adobe 5k [77], RAISE1k [78], DIV2K [79], Davis Middlebury [80], video deblurring [81], and ImageNet [15] datasets as well as a host of distortions of those same patches. The many distortion methods used are split into six different categories: (1) Traditional augmentation methods, outputs from (2) CNN-based autoencoders, (3) superresolution, (4) frame interpolation, (5) video deblurring, and (6) colorization. The BAPPS dataset consists of two sets with different labels and intended use, Two Alternative Forced Choice (2AFC) and Just Noticeable Differences (JND).

2AFC consists of image patches and two distorted versions of each patch, as well as human annotations as to which distorted patch is most similar to the original. The aim of 2AFC is to train and evaluate models for perceptual similarity judgment by evaluating if those models give higher similarity to the distortion that most human annotators agreed was more similar.

JND consists of image patches, a barely distorted version of each patch, as well as human annotations of whether the two patches are the same. The human annotators were shown the two images only briefly and were also shown pairs of the same and very different images. The aim of JND is to test models for perceptual similarity by evaluating if those models give a higher similarity to those samples that human annotators had difficulty telling apart. JND is purely used for model testing and the model is assigned a score based on how well it ranks the image pairs by similarity in comparison to the similarity ranking derived from the fraction of humans that thought they were the same.

2AFC is split into a training and testing part while JND is used solely for testing. How these are split between training and testing as well as different distortion categories can be found in Table III. In this regard, the JND part acts like a sentinel task for the 2AFC part by being used to verify whether there is a correlation between models that perform well on one perceptual similarity task to another.

V. LOSS NETWORKS AND FEATURE EXTRACTION

The primary goal of this work is to explore how using different pretrained architectures and feature extraction points affects the implemented experiments. For each of the four experiments, the same pretrained architectures and feature extraction points have been used. This section details how feature extraction is performed from the different networks and why those particular extraction points were chosen. A summary of the pretrained networks used and at which points features are extracted is detailed in Table IV.

The loss networks used for the experiments are created by selecting an architecture and a feature extraction point. A model of the selected architecture pretrained on ImageNet is then collected and layers after the extraction point are removed, and the output of the loss network is the features extracted at the selected point. How these features are used is described in the Experimental Details section.

As one of the objectives of this work is to evaluate where to perform feature extraction, the extraction points have been distributed throughout the network. Furthermore, the extraction points have been limited to the convolutional layers of the networks as these are typically used for deep perceptual loss. Additionally, the convolutional layers benefit from having no upper limit to the size of the input images, while using later layers typically requires the use of an exact input size.

Since testing all available extraction points would require a computation load that is unjustifiable for this work, four points were chosen for each network. The points were chosen such that they represent points that are early, semi-early, middle, and late in the convolutional layers. Additionally, for architectures of similar design, the extraction points are chosen such that they represent the "same" points in each network. For example, in the residual networks, the extraction points are after the first ReLU as well as after the same block stacks with the difference that each residual network architecture has a varying number of layers in the different block stacks.

VI. EXPERIMENTAL DETAILS

This section details the experiments that were performed in this work. The experiments mostly follow the procedures of the baseline papers as described in Section III with additional loss networks tested. The additional loss networks used are those presented in Table IV pretrained on ImageNet with feature extraction at the defined points. In all experiments four loss networks for each architecture are tested, each using one of the four feature extraction points defined for that architecture. For each experiment, some performance metrics are defined, and these metrics are used to evaluate the various loss networks for that task.

To accommodate the experiments, some parts of the baselines were changed or not used and those differences will be detailed here. For complete and in-depth details of the experiments, it is recommended to read the baseline papers.

A. Experiments Based on Paper 1

The experiments replicate those in Paper 1 with a few changes, besides the changes in loss networks.

TABLE IV
LOSS NETWORK ARCHITECTURES AND FEATURE EXTRACTION POINTS

Architecture	Feature Extraction Points
<i>VGG Networks</i>	
VGG-11 [45]	1st, 2nd, 4th, and 8th ReLU
VGG-16 [45]	2nd, 4th, 7th, and 13th ReLU
VGG-16_bn [45]	2nd, 4th, 7th, and 13th ReLU
VGG-19 [45]	2nd, 4th, 8th, and 16th ReLU
<i>Residual Networks</i>	
ResNet-18 [46]	1st ReLU, 1st, 2nd, and 4th Block Stack
ResNet-50 [46]	1st ReLU, 1st, 2nd, and 4th Block Stack
ResNeXt-50 32x4d [47]	1st ReLU, 1st, 2nd, and 4th Block Stack
<i>Inception Networks</i>	
GoogLeNet [48]	1st BN, 1st, 3rd, and 9th Inception Module
InceptionNet v3 [49]	3rd BN, 1st, 3rd, and 8th Inception Module
<i>EfficientNet</i>	
EfficientNet_B0 [50]	1st SiLU, 1st, 4th, and 7th MBConv
EfficientNet_B7 [50]	1st SiLU, 1st, 4th, and 7th MBConv
<i>Uncategorized Networks</i>	
AlexNet [51]	1st, 2nd, 3rd, and 5th ReLU
DenseNet-121 [52]	1st ReLU, 1st, 2nd, and 4th Dense Block
SqueezeNet 1.1 [53]	1st ReLU, 1st, 4th, and 8th Fire Module

Only the experiments where image-to-image autoencoders trained with deep perceptual loss were replicated. The experiments using pixel-wise and feature prediction loss were excluded as they are not the topic of this work. The experiments using feature-to-image autoencoders were excluded as they consistently performed slightly worse than their image-to-image counterparts.

As the experiments as originally presented are computationally expensive, especially when repeating the experiments for many different loss networks, some steps have been taken to reduce the computational needs. The number of epochs used in training has been reduced from 50 to 10 for autoencoders and 500 to 200 for MLPs. It was verified that this did not have a significant impact on the results by also running a part of the experiments with unchanged epochs and comparing the results. Additionally, the encoding size (z) was fixed to 64 for the experiments.

Only two of the three datasets tested in the original work have been evaluated here. *i.e.*, SVHN and STL-10, as the third dataset, LunarLander-v2 [59] Collection, is cumbersome to generate, computationally expensive to train on, and has not been used in that fashion by any other works. Like in Paper 1, this work does not follow the STL-10 standard testing procedure. Instead 80% of the training set is used for MLP training and 20% for validation. For Experiment 1 the performance metrics used are the downstream test set accuracy on SVHN and STL-10.

B. Experiments Based on Paper 2

Experimentation strategy and evaluation metrics are followed from Paper 2, and precisely, the Massachusetts Roads Dataset (MRD) [64] is chosen to explore further. Extended experiments are conducted with the multiple architectures and feature

extraction points mentioned in Table IV. While the iterative refinement is adapted from the original work with many iterations ranging from 1 to 3, whereas the input patch size was resized to 224×224 for computational efficiency. In the original paper, details of training epochs remain unclear, so all the experiments were performed for 100 epochs. The performance metrics for Experiment 2 are the same as in the original work completeness, correctness, and quality of road extraction as defined in [62].

C. Experiments Based on Paper 3

While Paper 3 investigates both super-resolution and style transfer, the latter is left out in this work due to lacking direct evaluation metrics. A similar experimental process as in the paper is followed for super-resolution, using the same architecture and parameter values for the task of super-resolution for factors $\times 4$ and $\times 8$. In this work, training is done using 10K images from the MSCOCO 2014 training set using a specific seed for reproducibility purposes in future research. The original paper performs training for 200K iterations, but it is unclear whether there is some validation or which model is finally kept for inference. In the preliminary experiments, several architectures collapsed in the final epochs and produce black images. Thus, in the final experiments, the models are trained for the same number of iterations with an additional evaluation step in every epoch to keep the best model according to the PSNR metric on 100 images from the MSCOCO 2014 validation set. The performance metrics for Experiment 3 are the PSNR and MSSIM scores for Set 5, Set 14, and BSD100 for $\times 4$ and $\times 8$ upscaling.

D. Experiments Based on Paper 4

This work only performs the experiments in Paper 4 that use ImageNet pretrained networks with all importance weights set to 1 and without additional training. In essence, this means that each loss network is evaluated for how well it performs as a perceptual metric on the BAPPS dataset. For Experiment 4 the performance metrics used are the 2AFC score and mAP% on the JND dataset. The 2AFC score is also recorded for the individual subsets of the 2AFC part, but they are not used as performance metrics as they are included in the full 2AFC score.

VII. RESULTS AND ANALYSIS

The performance metrics on the four experiments have been analyzed together with a host of different attributes to attempt to provide insights into how to decide which architecture to choose and what layers to extract features from. The attributes that have been analyzed can be split into those that depend only on the architecture and those that depend on the architecture and extraction point. The attributes that depend on the architecture are, ImageNet accuracy, number of parameters, depth¹, flops in the forward pass, and whether the architectures

¹Depth is measured as the maximum number of non-linearly separated matrix multiplications up to the given point (*i.e.*, if the architecture branches and then rejoins only the longest branch is counted).

uses skip-connections, branching, 1×1 -convolutions, or batch normalization. The attributes that also depend on the extraction point are the number of parameters, depth, and compute before the extraction point as well as the number of features and channels at the extraction point. Additionally, some attributes derived from these were used, such as the fraction of the architecture's total parameters that exist up until the extraction points. Finally, the performance metrics of the four experiments were compared with each other to identify potential task-independent trends.

A large amount of data has been gathered from several evaluations over the four experiments, which is unwieldy to include in a paper in its entirety. For this reason, the raw data and attributes have been relegated to supplementary material for those that wish to make a deeper examination. More information about the supplementary material, including how to easily access the raw data and quickly generate scatterplots of attributes and performance metrics can be found in the Appendix. This section presents the data of general interest such as indications of trends or lack thereof.

From the data gathered three primary findings related to how to select a loss network were identified. Those three findings are summarized below and then expanded on in their respective subsections.

- 1) Using the correct extraction point is at least as important as selecting the architecture.
- 2) In general, the non-batch normalized VGG networks and SqueezeNet perform well for most tasks if the correct layers are used.
- 3) There is no simple correlation between an architecture's performance on ImageNet and its performance as a loss network.

Furthermore, some correlations which are typically assumed in the field of transfer learning were not observed. The analysis of the implications of these results is further expanded in the Discussion section.

A. Selecting Extraction Point

The selection of where the features used for loss calculation are extracted in the network has a huge impact on the performance across all performance metrics and architectures. For all performance metrics, selecting the best extraction point of the worst architecture will give around the same performance as selecting the worst extraction point of the best architecture. This shows that selecting the extraction point for the loss network is as significant as selecting which model to use. In Table V the best layer for each architecture is shown for some performance metrics of each experiment. The architecture with the best performance for the performance metric is underlined. In Figure 2 the performance of each architecture is shown for all their extraction points for some of the performance metrics.

Interestingly, for most performance metrics the extraction point which performs best is similar across architectures. This indicates that the selected extraction points are roughly equivalent which is desired and reinforces the existing consensus that two deep networks will learn similar features at similar points along their depth. However, the spread of which extraction

TABLE V
THE BEST LAYER OF EACH ARCHITECTURE FOR SOME DATASETS OF EACH EXPERIMENT

Architecture	Best layer per performance metric (E: Early, S: Semi-Early, M: Mid, L: Late)						
	A		B	C		D	
	SVHN	STL-10	MRD (All)	4x MSSIM BSDS100	8x MSSIM BSDS100	2AFC	JND
<i>VGG Networks</i>							
VGG-11 [45]	M	L	L	<u>E</u>	E	L	<u>L</u>
VGG-16 [45]	M	<u>L</u>	E	E	E	L	L
VGG-16_bn [45]	M	L	S	M	E	L	L
VGG-19 [45]	<u>M</u>	L	<u>M</u>	E	E	L	L
<i>Residual Networks</i>							
ResNet-18 [46]	M	S	M	E	E	L	L
ResNet-50 [46]	M	S	E	S	E	S	L
ResNeXt-50 32x4d [47]	M	M	M	E	E	L	L
<i>Inception Networks</i>							
GoogLeNet [48]	S	L	L	E	E	M	L
InceptionNet v3 [49]	S	M	L	S	M	S	S
<i>EfficientNet</i>							
EfficientNet_B0 [50]	M	L	L	S	S	M	M
EfficientNet_B7 [50]	M	M	L	S	E	M	M
<i>Uncategorized Networks</i>							
AlexNet [51]	E	L	L	E	E	<u>M</u>	L
DenseNet-121 [52]	M	L	L	M	E	M	L
SqueezeNet 1.1 [53]	S	L	L	E	<u>E</u>	M	L

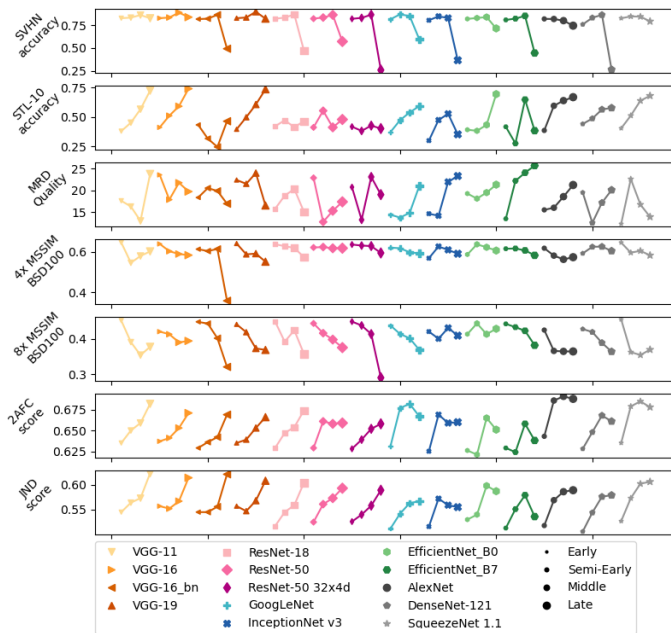


Fig. 2. The results of each loss network ordered by extraction point (earliest to latest) for some performance metrics for each experiment.

points give the best performance on the different performance metrics goes against the common practice of using the last or later layer for feature extraction. For a majority of architectures, the earliest extraction point is the best for the super-resolution experiments (Paper 3) on all performance metrics, while the

last extraction point gives the highest downstream accuracy on STL-10 (Paper 1).

So, while there exists some agreement between architectures as to which extraction point to use, that point depends on the task and dataset. While the gathered data does not give a conclusive way to predict which extraction point will be best for a given task and dataset, there are some trends.

Selecting an extraction point for a loss network determines what features will be compared during the calculation of loss or similarity. When optimizing the loss, the output will trend towards an image that gives rise to similar activations at the extraction point. Deeper layers of networks are known to represent higher-level features, so the extraction point directly affects which type of features will be emphasized in image generation. Extracting from early layers means that the smaller pixel level patterns affect loss more while from later layers means that the general content and structure of the image affect the loss more. Whether it is best to optimize images on lower or higher-level features depends on the task. For example, in the super-resolution experiments (Paper 3) for all three test datasets, the optimal extraction point was early. Since super-resolution is a task where the individual pixels matter a lot, it is not unexpected that earlier extraction points that are focused on low-level features are best.

For the task of training an autoencoder for downstream predictions (Paper 1) later extraction points perform better. Likely this is due to classification tasks relying on higher-level features which means that autoencoders trained to replicate images that are similar in the later layers, would therefore also encode information relevant to higher-level features. The

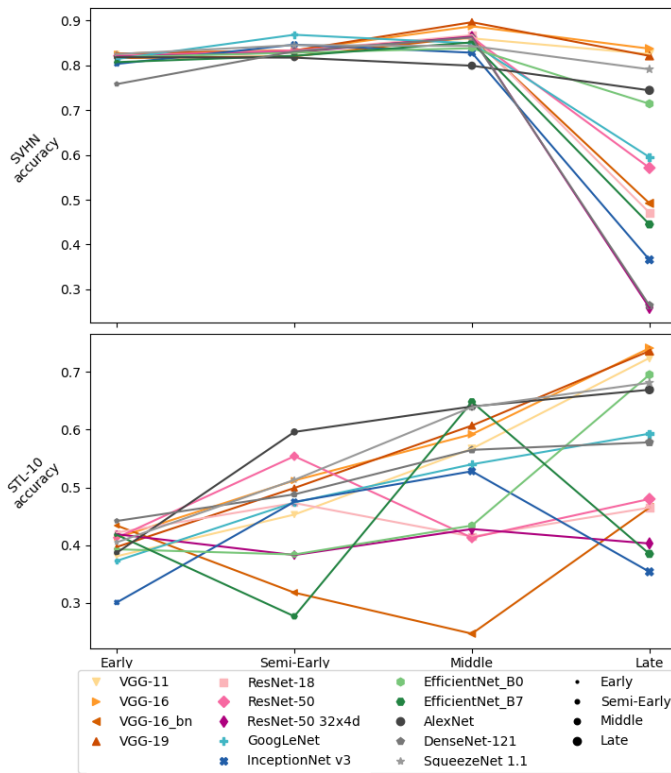


Fig. 3. The performance of all loss networks on SVHN and STL-10 where each loss network has been grouped by its extraction point. More figures like these can be quickly generated in the supplementary spreadsheet, using any combination of investigated attributes and performance metrics.

difference between the two evaluated datasets, SVHN and STL-10, is also noteworthy. For SVHN accuracy most architectures performed the best using the middle extraction point, compared to STL-10 accuracy for which the late extraction point was preferred. This difference is visualized in Fig. 3 which shows the performance of the different loss networks, grouped by extraction point, on the two datasets. This is notable since STL-10 is derived from a subset of ImageNet. SVHN on the other hand is the adjusted close-up images of house number digits, which are different from the typical photos in the ImageNet dataset. This also fits into the idea that the extraction point should match the task since the features in the later layers are expected to be more specific to the pretraining dataset and therefore more useful for extracting features of a similar dataset. When selecting an extraction point it is therefore worth considering how similar the dataset is to the one used for pretraining the loss networks.

Another consideration when selecting an extraction point (and architecture) is the computational demands during training. Some of the architectures that were evaluated require high amounts of computation on top of that required for the model that is being trained. For training smaller models this could potentially increase the computation power needed to train an order of magnitude. Using earlier extraction points means smaller loss networks, which reduce this additional computation. Taking into account that the later extraction points do not always perform better, this makes the argument for using earlier

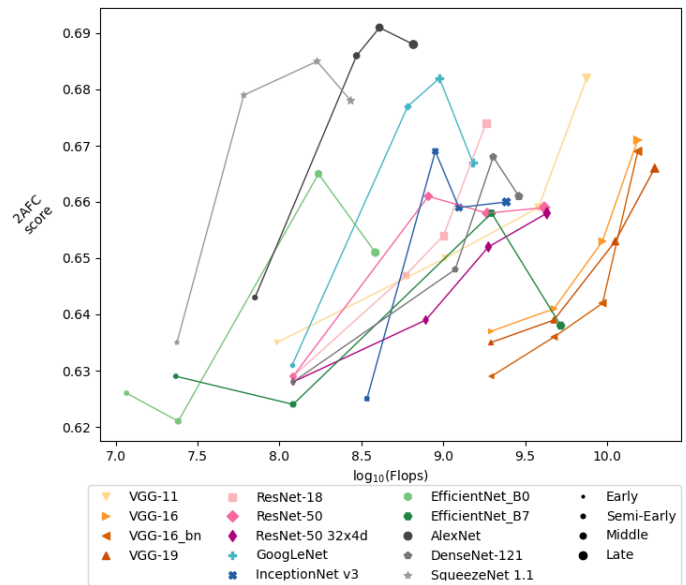


Fig. 4. The performance of all loss networks on the 2AFC split of BAPPS compared to the \log_{10} amount of flops in a forward pass of that loss network.

extraction points stronger. This is illustrated in Fig. 4 where, for each loss network, the 2AFC score is plotted against the \log_{10} amount flops for the forward pass. It is clear that selecting an earlier extraction point can potentially reduce the computation requirements by orders of magnitude.

B. Selecting architecture

To gain insight into what architecture attributes are beneficial for a loss network, the performance of each architecture is analyzed. In Table VI, a summary of each architecture's performance is presented. For each performance metric, the architectures are ranked according to the performance of the best extraction point between 1 (best) and 14 (worst). The table presents the average ranking of each architecture per paper as well as the overall average (each paper is weighted equally).

Across all four papers two VGG networks without batch-norm place in the top three when averaging the rankings of all performance metrics (when the best extraction point is used for all networks). Interestingly the batch-normalized VGG-16 network places in the bottom four on all tasks except perceptual similarity (Paper 4). The only network besides the VGG networks that do not use batch-norm is AlexNet, which gets an average of 8th place over all four papers. Another architecture that performs well is SqueezeNet which has an average performance on the autoencoder training (Paper 1) and delineation (Paper 2) experiments but is second best at perceptual similarity (Paper 4) and the best at super-resolution (Paper 3). SqueezeNet is also a good option in all experiments when looking for performance as well as low computational needs. It is also worth noting that besides adding batch-norm to VGG, the architectures within the same basic template (VGGs, ResNets, and EfficientNets) perform similarly, with little indication of which would be the better choice.

TABLE VI
RANKINGS OF THE BEST LOSS NETWORK FOR EACH ARCHITECTURE ON
THE PERFORMANCE METRICS AVERAGED PER EXPERIMENT

Architecture	Average ranking per experiment				
	A	B	C	D	All
<i>VGG Networks</i>					
VGG-11 [45]	6.0	2.67	2.33	2.5	3.38
VGG-16 [45]	1.5	3.67	6.75	4.5	4.10
VGG-16_bn [45]	9.5	11.33	11.08	4.5	9.10
VGG-19 [45]	1.5	1.67	4.25	7.0	3.60
<i>Residual Networks</i>					
ResNet-18 [46]	8.0	12.67	7.08	5.5	8.31
ResNet-50 [46]	8.5	6.67	7.33	10.0	8.13
ResNeXt-50 32x4d [47]	9.5	5.67	5.67	11.5	8.08
<i>Inception Networks</i>					
GoogLeNet [48]	5.5	10.33	9.67	8.5	8.50
InceptionNet v3 [49]	11.0	4.67	11.83	10.5	9.50
<i>EfficientNet</i>					
EfficientNet_B0 [50]	8.5	11.67	9.92	9.0	9.77
EfficientNet_B7 [50]	8.5	3.00	8.83	12.5	8.21
<i>Uncategorized Networks</i>					
AlexNet [51]	10.0	9.33	8.58	5.0	8.23
DenseNet-121 [52]	8.5	13.67	10.50	10.5	10.79
SqueezeNet 1.1 [53]	8.5	8.00	1.17	3.5	5.29

C. Loss network performance vs. ImageNet accuracy

For the architectures and extraction points tested in this work there does not seem to be any strong correlation between the ImageNet accuracy of the loss network and the downstream performance of the models trained with them. The positive linear correlation between ImageNet accuracy and downstream performance that is often expected in computer vision transfer learning was absent in all experiments. This has previously been shown to hold for deep perceptual similarity [27], and now also seems to hold for deep perceptual loss. However, the upper bound of perceptual similarity as a function of ImageNet performance that was reported in that work has not been replicated or refuted for deep perceptual loss. It would likely require an evaluation of orders of magnitude more loss network to do so. The performance of the best loss network for each architecture on MRD Quality compared to the ImageNet top-1 accuracy is shown in Fig. 5.

VIII. DISCUSSION

The discussion is split into four parts. The first subsection deals with the direct implications of the results. The second covers what remains uncertain. The third details the potential flaws in this work. The final subsection discusses the impact of this work on the field from a higher level.

A. Implications of the study

Some of the most novel finds of this work come from the impact of extraction point selection on performance. This is not surprising since the extraction point selection has not been well-explored when it comes to deep perceptual loss and, arguably,

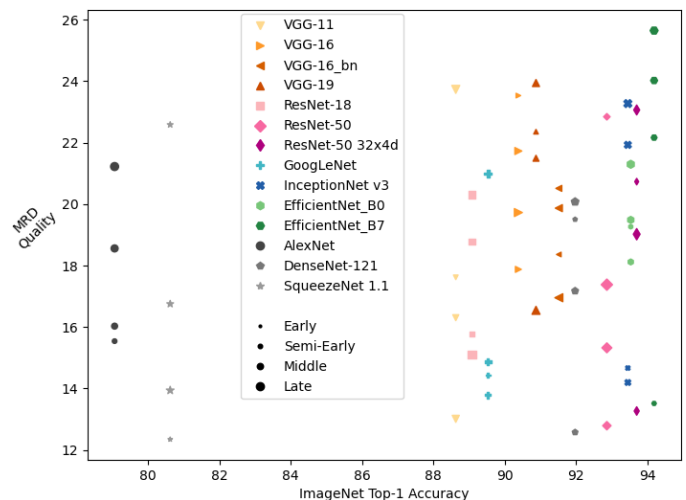


Fig. 5. The MRD Quality performance of each loss network compared to the ImageNet top-1 accuracy or the pretrained models.

feature learning in general. It is clear that if one architecture performs better with a certain extraction point another will likely also have a relatively good performance for an equivalent extraction point. Additionally, it can be inferred from the task and dataset which extraction points will likely perform better. Such inference is best made by considering exactly what deep features are compared and what it means to minimize that comparison. However, a simple rule-of-thumb that likely works well is to use earlier layers when the downstream task depends more on local structures or when the task dataset is dissimilar to the training dataset.

Another inference that can be made is that VGG networks are a good choice of network for most tasks. What is difficult to tell is why the VGG networks are successful. They are some of the least complex architectures tested and together with AlexNet the only networks that do not (necessarily) use batch-norm. Architectures with batch-norm also seem more susceptible to having extraction points for which the performance collapses in Experiments 1 and 3. However, it is not possible from the results to say if including batch-norm layers is in itself bad for loss networks. There could be other factors that make the VGG networks strong and the poor performance of VGG-16_bn might be specific to that architecture. Additionally, in Torchvision the models with batch-norm use a different pretraining procedure than those without, specifically they use a larger learning rate. This means that even if there was a clear difference between the architectures with and without batch-norm, this difference might be due to the training procedure rather than the architecture itself. These thoughts are expanded on in the next subsection.

Some of the explored attributes have no clear correlation to the performance metrics. The next subsection will discuss those attributes where the lacking correlation might be found by further experiments, but for the others, it seems unlikely that a simple correlation would exist at all. First among these is the lack of linear correlation between ImageNet Accuracy and improved performance. This generalizes some of the findings

from [27] about deep perceptual similarity to also apply to deep perceptual loss. Though, to expand the results from showing no linear correlation to show whether the threshold value for optimal performance also holds would require an order of magnitude more experiments. It is not surprising that these results generalized as deep perceptual loss can be seen as an application of deep perceptual similarity. Other architecture-specific attributes, such as total depth and the total number of parameters in the network, showed similar trends as ImageNet accuracy. No clear correlations can be shown and if any correlations do exist, they would be complex and likely require at least an order of magnitude more experiments to appear. Interestingly this means that there is no clear correlation between the total depth of a network and how useful its features are for deep perceptual loss. It is typically expected that, given enough data, deeper networks should perform better on tasks they were trained directly on. Since depth is correlated with ImageNet accuracy, but seemingly not with perceptual similarity, this might be part of the reason why ImageNet accuracy and perceptual similarity have such an odd correlation. In [27] it is shown that the perceptual similarity scores of shallower architectures do not decay as much with increased ImageNet accuracy as their deeper counterparts.

The attributes that depend on both architecture and extraction point, such as the number of parameters up until the extraction point or the number of channels at the extraction point, do correlate to performance on individual performance metrics. However, these attributes also correlate with the depth of the extraction point and it is likely that the correlations were caused by each task's optimal extraction point. While attributes such as the number of channels at the extraction point do not have to correlate with depth, standard practices of architecture design mean they still do for the evaluated architectures.

B. Open questions

This work reveals some trends that can be used to improve extraction points selection and these trends likely generalize beyond the experiments in this work. Such general trends have not been observed when it comes to the choice of architecture. While the VGG networks without batch-norm were shown to be good choices, these findings do not generalize to architectures beyond those that have been evaluated.

One general problem with trying to show which factors of a neural network architecture correlate with performance is that for a given architecture many different models with varying performance can be trained. This issue cannot be solved by standardizing training since it would benefit the architectures better suited to the chosen training procedure. Instead, correlations can be found with aggregations of performance over multiple models of the given architecture. For example, in [27] the threshold value of ImageNet accuracy for performance on perceptual similarity is found only when considering the best networks for a given ImageNet accuracy. The models that are used in this work have already been pretrained which means that only a single model of each architecture is used. However, the models that are used can be considered to have already been aggregated since the available pretrained models

have already been selected for high ImageNet accuracy for the given architecture. In machine learning in general this type of aggregation is assumed when analyzing results. When the state-of-the-art results of an architecture are presented it is implied that the results refer to the best-achieved results with that architecture. Though, good practice dictates that the results are usually presented as the average accuracy of models trained with the best procedure found for a given architecture.

Interestingly, there are no strong correlations for performance metrics between different experiments. While some architectures like VGG without batch-normalizing generally perform well, others like SqueezeNet vary heavily between experiments. For a given performance metric, there is a tendency for certain extraction points to work better for all but some architectures, but for another performance metric, the architectures that break the pattern may vary with no consistency within the architecture for whether later or earlier points are better. In summary, the performance of a loss network in one experiment does not, in general, predict its performance in another.

C. Flaws in the study

The findings of this work are limited by a number of factors. The limited number of architectures tested is likely one of the reasons why no conclusion can be drawn relating to some attributes. The datasets used were mostly limited, especially within tasks, leading to the interpretations related to changing datasets being weak. The selected extraction points for each architecture are assumed to be equivalent, however, this might not be the case. Some architectures might perform worse simply due to the features at the selected extraction points being unsuitable for the tasks. Additionally, in transfer learning settings it is commonly held that slight differences in extraction points only lead to minor changes in performance, especially if fine-tuning is used [82]. This reasoning might extend to deep perceptual loss as well, though further study would be needed.

Another potential problem with the work is the performance metrics used for Experiment 3. PSNR and MSSIM are similarity metrics comparing the upscaled image and the true image. The performance metrics used here are PSNR and MSSIM, the same as in Paper 3. However, these metrics have been called into question when it comes to how well they represent the human perception of similarity [12]. This shortcoming is also noted in Paper 3, where the use of the metrics is justified as a way to show the difference between different types of loss rather than an attempt at showing state-of-the-art performance. In addition to this, it could be argued that performing well on both of these metrics might be a good indicator of quality even if it does not correlate directly with human perception of quality. Though, it is likely that the preference for earlier extraction points in these experiments is due to using metrics that compare local and low-level features. The obvious alternatives to using such metrics would be to use deep perceptual similarity or human judgments, the former of which will bias the results towards the loss network chosen for similarity and the latter of which is expensive. Interestingly, there is no correlation between performance on the super-resolution subset of BAPPS and performance on the super-resolution metrics in Experiment 3,

which seem to further indicate that the low-level metrics used do not correspond well to human perceptions of quality.

D. Impact on the field

A lot of the questions regarding the architecture attributes that remain unanswered could likely better be addressed through an extensive ablation study. However, it is also worth considering if this would be a productive use of scientific resources considering the size of the subfield. A more valuable use of resources might be to perform such an ablation study for more established transfer learning approaches. The findings of such a study might then be extended to the subfield of deep perceptual similarity and loss at a lower cost.

The broader field of transfer learning is filled with assumptions, conventions, and accepted good practices. Many of these are backed by solid studies, others are interpretations of trends observed over many papers without cohesive methodologies. One convention is to do feature extraction, retraining, or adding new layers at the last layer or after the last convolutional layer of the pretrained architecture. This practice has not been as prevalent for deep perceptual loss and this work demonstrates clearly that it is not necessarily the best practice for this purpose either. It is possible that extracting from the later layers might be a flawed practice also within the larger field of transfer learning. A study of common transfer learning settings that focuses on the correlations between downstream transfer learning performance and feature extraction points could prove useful.

Another part of the transfer learning field that is in need of investigation is the assumption that better ImageNet accuracy leads to better downstream transfer learning performance. While [27] showed that this assumption does not hold for deep perceptual similarity, to do this thousands of networks were trained and analyzed in depth. However, no systematic analysis of the correlation of ImageNet accuracy to downstream transfer learning performance has been found. The assumption is instead backed by trends from disparate application-oriented papers. It is possible that the threshold ImageNet accuracy for optimal performance also holds for other transfer learning tasks. If this is the case it likely requires the evaluation of many models to confirm. In short, it is high time to confirm or reject the generally accepted principle that pretraining performance on ImageNet correlates positively with downstream performance in common transfer learning settings. Ideally, this would be achieved through an extensive systematic study.

IX. CONCLUSION

Large-scale systematic testing and analysis of loss networks with varying architectures and extractions points have been performed. The results and analysis point to the three primary findings. First, selecting the extraction point for features is at least as important as selecting the architecture and good practice for making this selection is suggested. Secondly, while no general rule for selecting architecture could be identified, the non-batch normalized VGG networks are a good choice. Thirdly, there is no simple correlation between architecture attributes such as ImageNet accuracy, depth, and the number

of parameters and downstream performance when used as a loss network.

The results also reinforce and expand earlier works showing that two established conventions within the field of transfer learning do not apply to deep perceptual loss and similarity. The conventions in question are that the final layers are the best candidates for feature extraction and that better ImageNet accuracy implies better downstream transfer learning performance. Furthermore, these conventions are called into question for the entire field of transfer learning with extensive studies recommended to finally confirm or reject them.

ACKNOWLEDGMENT

This work required a lot of computation to complete, which was provided through the GPU data lab of Luleå University of Technology.

We would also like to thank Christian Günther for help with setting up the coding and execution environments that were used for many of the experiments.

REFERENCES

- [1] C. Szegedy, W. Zaremba, I. Sutskever, J. Bruna, D. Erhan, I. Goodfellow, and R. Fergus, "Intriguing properties of neural networks." arXiv, 2013. [Online]. Available: <http://arxiv.org/abs/1312.6199>
- [2] I. Goodfellow, J. Pouget-Abadie, M. Mirza, B. Xu, D. Warde-Farley, S. Ozair, A. Courville, and Y. Bengio, "Generative adversarial nets," in *Advances in neural information processing systems*, 2014, pp. 2672–2680. [Online]. Available: <https://doi.org/10.1145/3422622>
- [3] J. Yosinski, J. Clune, A. M. Nguyen, T. J. Fuchs, and H. Lipson, "Understanding neural networks through deep visualization." arXiv, 2015. [Online]. Available: <https://arxiv.org/abs/1506.06579>
- [4] Z. Cheng, Q. Yang, and B. Sheng, "Deep colorization," in *Proceedings of the IEEE International Conference on Computer Vision (ICCV)*, December 2015.
- [5] L. A. Gatys, A. S. Ecker, and M. Bethge, "Image style transfer using convolutional neural networks," in *Proceedings of the IEEE Conference on Computer Vision and Pattern Recognition (CVPR)*, June 2016.
- [6] A. B. L. Larsen, S. K. Sønderby, H. Larochelle, and O. Winther, "Autoencoding beyond pixels using a learned similarity metric," in *Proceedings of The 33rd International Conference on Machine Learning*, ser. Proceedings of Machine Learning Research, vol. 48. PMLR, June 2016, pp. 1558–1566. [Online]. Available: <https://proceedings.mlr.press/v48/larsen16.html>
- [7] J. Johnson, A. Alahi, and L. Fei-Fei, "Perceptual losses for real-time style transfer and super-resolution," in *European conference on computer vision*. Springer, 2016, pp. 694–711. [Online]. Available: https://doi.org/10.1007/978-3-319-46475-6_43
- [8] Q. Yang, P. Yan, Y. Zhang, H. Yu, Y. Shi, X. Mou, M. K. Kalra, Y. Zhang, L. Sun, and G. Wang, "Low-dose CT image denoising using a generative adversarial network with wasserstein distance and perceptual loss,"

- IEEE Transactions on Medical Imaging*, vol. 37, no. 6, pp. 1348–1357, 2018.
- [9] Z. Chai, K. Zhou, J. Yang, Y. Ma, Z. Chen, S. Gao, and J. Liu, “Perceptual-assisted adversarial adaptation for choroid segmentation in optical coherence tomography,” in *2020 IEEE 17th International Symposium on Biomedical Imaging (ISBI)*, 2020, pp. 1966–1970.
- [10] G. G. Pihlgren, F. Sandin, and M. Liwicki, “Improving image autoencoder embeddings with perceptual loss,” in *2020 International Joint Conference on Neural Networks (IJCNN)*, 2020, pp. 1–7.
- [11] X. Liu, H. Gao, and X. Ma, “Perceptual losses for self-supervised depth estimation,” *Journal of Physics: Conference Series*, vol. 1952, no. 2, p. 022040, jun 2021. [Online]. Available: <https://dx.doi.org/10.1088/1742-6596/1952/2/022040>
- [12] R. Zhang, P. Isola, A. A. Efros, E. Shechtman, and O. Wang, “The unreasonable effectiveness of deep features as a perceptual metric,” in *Proceedings of the IEEE conference on computer vision and pattern recognition*, 2018, pp. 586–595.
- [13] S. Marcel and Y. Rodriguez, “Torchvision the machine-vision package of torch,” in *Proceedings of the 18th ACM International Conference on Multimedia*, ser. MM ’10. Association for Computing Machinery, 2010, p. 1485–1488. [Online]. Available: <https://doi.org/10.1145/1873951.1874254>
- [14] A. Paszke, S. Gross, F. Massa, A. Lerer, J. Bradbury, G. Chanan, T. Killeen, Z. Lin, N. Gimelshein, L. Antiga, A. Desmaison, A. Kopf, E. Yang, Z. DeVito, M. Raison, A. Tejani, S. Chilamkurthy, B. Steiner, L. Fang, J. Bai, and S. Chintala, “PyTorch: an imperative style, high-performance deep learning library,” in *Advances in Neural Information Processing Systems 32*, H. Wallach, H. Larochelle, A. Beygelzimer, F. d’Alché-Buc, E. Fox, and R. Garnett, Eds. Curran Associates, Inc., 2019, pp. 8024–8035.
- [15] J. Deng, W. Dong, R. Socher, L.-J. Li, K. Li, and L. Fei-Fei, “ImageNet: a large-scale hierarchical image database,” in *2009 IEEE Conference on Computer Vision and Pattern Recognition*, 2009, pp. 248–255.
- [16] G. Farias, S. Dormido-Canto, J. Vega, G. Rattá, H. Vargas, G. Hermosilla, L. Alfaro, and A. Valencia, “Automatic feature extraction in large fusion databases by using deep learning approach,” *Fusion Engineering and Design*, vol. 112, pp. 979–983, 2016.
- [17] G. E. Hinton, S. Osindero, and Y.-W. Teh, “A fast learning algorithm for deep belief nets,” *Neural computation*, vol. 18, no. 7, pp. 1527–1554, 2006.
- [18] H. Lee, A. Battle, R. Raina, and A. Ng, “Efficient sparse coding algorithms,” *Advances in neural information processing systems*, vol. 19, 2006.
- [19] Q. V. Le, “Building high-level features using large scale unsupervised learning,” in *2013 IEEE international conference on acoustics, speech and signal processing*. IEEE, 2013, pp. 8595–8598.
- [20] G. E. Hinton and R. R. Salakhutdinov, “Reducing the dimensionality of data with neural networks,” *science*, vol. 313, no. 5786, pp. 504–507, 2006.
- [21] Y. Bengio, P. Lamblin, D. Popovici, and H. Larochelle, “Greedy layer-wise training of deep networks,” *Advances in neural information processing systems*, vol. 19, 2006.
- [22] Y. Hayakawa, T. Oonuma, H. Kobayashi, A. Takahashi, S. Chiba, and N. M. Fujiki, “Feature extraction of video using deep neural network,” in *2016 IEEE 15th International Conference on Cognitive Informatics & Cognitive Computing (ICCI* CC)*. IEEE, 2016, pp. 465–470.
- [23] S. H. Lee, C. S. Chan, S. J. Mayo, and P. Remagnino, “How deep learning extracts and learns leaf features for plant classification,” *Pattern Recognition*, vol. 71, pp. 1–13, 2017.
- [24] B. Jiang, J. Yang, Z. Lv, K. Tian, Q. Meng, and Y. Yan, “Internet cross-media retrieval based on deep learning,” *Journal of Visual Communication and Image Representation*, vol. 48, pp. 356–366, 2017.
- [25] H. Mohsen, E.-S. A. El-Dahshan, E.-S. M. El-Horbaty, and A.-B. M. Salem, “Classification using deep learning neural networks for brain tumors,” *Future Computing and Informatics Journal*, vol. 3, no. 1, pp. 68–71, 2018.
- [26] M. Alberti, M. Seuret, R. Ingold, and M. Liwicki, “A pitfall of unsupervised pre-training.” arXiv, 2017. [Online]. Available: <https://arxiv.org/abs/1703.04332>
- [27] M. Kumar, N. Houlsby, N. Kalchbrenner, and E. D. Cubuk, “On the surprising tradeoff between imagenet accuracy and perceptual similarity.” arXiv, 2022. [Online]. Available: <https://arxiv.org/abs/2203.04946>
- [28] J. Schmidhuber, “Learning Factorial Codes by Predictability Minimization,” *Neural Computation*, vol. 4, no. 6, pp. 863–879, 11 1992. [Online]. Available: <https://doi.org/10.1162/neco.1992.4.6.863>
- [29] K. Simonyan, A. Vedaldi, and A. Zisserman, “Deep inside convolutional networks: Visualising image classification models and saliency maps,” in *Workshop at International Conference on Learning Representations*, 2014.
- [30] A. Dosovitskiy and T. Brox, “Generating images with perceptual similarity metrics based on deep networks,” in *Advances in neural information processing systems*, 2016, pp. 658–666.
- [31] A. Mosinska, P. Marquez-Neila, M. Koziński, and P. Fua, “Beyond the pixel-wise loss for topology-aware delineation,” in *Proceedings of the IEEE conference on computer vision and pattern recognition*, 2018, pp. 3136–3145.
- [32] J. Li, X. Liang, Y. Wei, T. Xu, J. Feng, and S. Yan, “Perceptual generative adversarial networks for small object detection,” in *The IEEE Conference on Computer Vision and Pattern Recognition (CVPR)*, July 2017.
- [33] Z. Wang, A. Bovik, H. Sheikh, and E. Simoncelli, “Image quality assessment: from error visibility to structural similarity,” *IEEE Transactions on Image Processing*, vol. 13, no. 4, pp. 600–612, 2004.
- [34] H. Zhao, O. Gallo, I. Frosio, and J. Kautz, “Loss functions for image restoration with neural networks,” *IEEE Transactions on Computational Imaging*, vol. 3, no. 1, pp. 47–57, 2017.

- [35] J. Snell, K. Ridgeway, R. Liao, B. D. Roads, M. C. Mozer, and R. S. Zemel, "Learning to generate images with perceptual similarity metrics," in *2017 IEEE International Conference on Image Processing (ICIP)*, 2017, pp. 4277–4281.
- [36] M. Kettunen, E. Härkönen, and J. Lehtinen, "E-LPIPS: robust perceptual image similarity via random transformation ensembles." arXiv, 2019. [Online]. Available: <http://arxiv.org/abs/1906.03973>
- [37] D. Xu, Y. Wang, X. Zhang, N. Zhang, and S. Yu, "Infrared and visible image fusion using a deep unsupervised framework with perceptual loss," *IEEE Access*, vol. 8, pp. 206 445–206 458, 2020.
- [38] C. Ledig, L. Theis, F. Huszár, J. Caballero, A. Cunningham, A. Acosta, A. Aitken, A. Tejani, J. Totz, Z. Wang *et al.*, "Photo-realistic single image super-resolution using a generative adversarial network," in *Proceedings of the IEEE conference on computer vision and pattern recognition*, 2017, pp. 4681–4690.
- [39] C. Shi and C.-M. Pun, "Adaptive multi-scale deep neural networks with perceptual loss for panchromatic and multispectral images classification," *Information Sciences*, vol. 490, pp. 1–17, 2019.
- [40] D. E. Rumelhart, G. E. Hinton, and R. J. Williams, "Learning internal representations by error propagation," California Univ San Diego La Jolla Inst for Cognitive Science, Tech. Rep., 1985.
- [41] D. H. Ballard, "Modular learning in neural networks." in *AAAI*, 1987, pp. 279–284.
- [42] D. P. Kingma and M. Welling, "Auto-encoding variational bayes." arXiv, 2013. [Online]. Available: <https://arxiv.org/abs/1312.6114>
- [43] Z. Wang, J. Chen, and S. C. H. Hoi, "Deep learning for image super-resolution: A survey," *IEEE Transactions on Pattern Analysis and Machine Intelligence*, vol. 43, pp. 3365–3387, 2021.
- [44] M. S. Rad, B. Bozorgtabar, U.-V. Marti, M. Basler, H. K. Ekenel, and J.-P. Thiran, "SROBB: targeted perceptual loss for single image super-resolution," in *Proceedings of the IEEE/CVF International Conference on Computer Vision (ICCV)*, October 2019.
- [45] K. Simonyan and A. Zisserman, "Very deep convolutional networks for large-scale image recognition," in *International Conference on Learning Representations*, 2015.
- [46] K. He, X. Zhang, S. Ren, and J. Sun, "Deep residual learning for image recognition," in *2016 IEEE Conference on Computer Vision and Pattern Recognition (CVPR)*, 2016, pp. 770–778.
- [47] S. Xie, R. Girshick, P. Dollár, Z. Tu, and K. He, "Aggregated residual transformations for deep neural networks," in *Proceedings of the IEEE conference on computer vision and pattern recognition*, 2017, pp. 1492–1500.
- [48] C. Szegedy, Wei Liu, Yangqing Jia, P. Sermanet, S. Reed, D. Anguelov, D. Erhan, V. Vanhoucke, and A. Rabinovich, "Going deeper with convolutions," in *2015 IEEE Conference on Computer Vision and Pattern Recognition (CVPR)*, 2015, pp. 1–9.
- [49] C. Szegedy, V. Vanhoucke, S. Ioffe, J. Shlens, and Z. Wojna, "Rethinking the inception architecture for computer vision," in *2016 IEEE Conference on Computer Vision and Pattern Recognition (CVPR)*, 2016, pp. 2818–2826.
- [50] M. Tan and Q. Le, "Efficientnet: Rethinking model scaling for convolutional neural networks," in *International Conference on Machine Learning*. PMLR, 2019, pp. 6105–6114.
- [51] A. Krizhevsky, "One weird trick for parallelizing convolutional neural networks." arXiv, 2014. [Online]. Available: <https://arxiv.org/abs/1404.5997>
- [52] G. Huang, Z. Liu, L. Van Der Maaten, and K. Q. Weinberger, "Densely connected convolutional networks," in *2017 IEEE Conference on Computer Vision and Pattern Recognition (CVPR)*, 2017, pp. 2261–2269.
- [53] F. N. Iandola, S. Han, M. W. Moskewicz, K. Ashraf, W. J. Dally, and K. Keutzer, "SqueezeNet: AlexNet-level accuracy with 50x fewer parameters and <0.5MB model size." arXiv, 2016. [Online]. Available: <https://arxiv.org/abs/1602.07360>
- [54] A. Krizhevsky, I. Sutskever, and G. E. Hinton, "ImageNet classification with deep convolutional neural networks," in *Advances in Neural Information Processing Systems* 25, F. Pereira, C. J. C. Burges, L. Bottou, and K. Q. Weinberger, Eds. Curran Associates, Inc., 2012, pp. 1097–1105.
- [55] K. De and M. Pedersen, "Impact of colour on robustness of deep neural networks," in *Proceedings of the IEEE/CVF International Conference on Computer Vision*, 2021, pp. 21–30.
- [56] G. G. Pihlgren, F. Sandin, and M. Liwicki, "Pretraining image encoders without reconstruction via feature prediction loss," in *2020 25th International Conference on Pattern Recognition (ICPR)*, 2021, pp. 4105–4111.
- [57] A. Coates, A. Ng, and H. Lee, "An analysis of single-layer networks in unsupervised feature learning," in *Proceedings of the fourteenth international conference on artificial intelligence and statistics*, 2011, pp. 215–223.
- [58] Y. Netzer, T. Wang, A. Coates, A. Bissacco, B. Wu, and A. Y. Ng, "Reading digits in natural images with unsupervised feature learning," in *NIPS Workshop on Deep Learning and Unsupervised Feature Learning 2011*, 2011.
- [59] G. Brockman, V. Cheung, L. Pettersson, J. Schneider, J. Schulman, J. Tang, and W. Zaremba, "OpenAI gym." arXiv, 2016. [Online]. Available: <https://arxiv.org/abs/1606.01540>
- [60] O. Ronneberger, P. Fischer, and T. Brox, "U-net: Convolutional networks for biomedical image segmentation," in *International Conference on Medical image computing and computer-assisted intervention*. Springer, 2015, pp. 234–241.
- [61] A. Sironi, E. Türetken, V. Lepetit, and P. Fua, "Multiscale centerline detection," *IEEE Transactions on Pattern Analysis and Machine Intelligence*, vol. 38, no. 7, pp. 1327–1341, 2015.
- [62] C. Wiedemann, C. Heipke, H. Mayer, and O. Jamet,

- “Empirical evaluation of automatically extracted road axes,” *Empirical evaluation techniques in computer vision*, vol. 12, pp. 172–187, 1998.
- [63] Q. Zou, Y. Cao, Q. Li, Q. Mao, and S. Wang, “CrackTree: automatic crack detection from pavement images,” *Pattern Recognition Letters*, vol. 33, no. 3, pp. 227–238, 2012.
- [64] V. Mnih, “Machine learning for aerial image labeling,” Ph.D. dissertation, University of Toronto, 2013.
- [65] I. Arganda-Carreras, S. C. Turaga, D. R. Berger, D. Cireşan, A. Giusti, L. M. Gambardella, J. Schmidhuber, D. Laptev, S. Dwivedi, J. M. Buhmann *et al.*, “Crowdsourcing the creation of image segmentation algorithms for connectomics,” *Frontiers in neuroanatomy*, p. 142, 2015.
- [66] L. A. Gatys, A. S. Ecker, and M. Bethge, “A neural algorithm of artistic style.” ArXiv, 2015. [Online]. Available: <https://arxiv.org/abs/1508.06576>
- [67] C. Dong, C. C. Loy, K. He, and X. Tang, “Image super-resolution using deep convolutional networks,” *IEEE transactions on pattern analysis and machine intelligence*, vol. 38, no. 2, pp. 295–307, 2015.
- [68] M. Bevilacqua, A. Roumy, C. Guillemot, and M.-L. Alberi-Morel, “Low-complexity single-image super-resolution based on nonnegative neighbor embedding,” in *BMVC*, 2012.
- [69] R. Zeyde, M. Elad, and M. Protter, “On single image scale-up using sparse-representations,” in *Curves and Surfaces*, 2010.
- [70] J.-B. Huang, A. Singh, and N. Ahuja, “Single image super-resolution from transformed self-exemplars,” *2015 IEEE Conference on Computer Vision and Pattern Recognition (CVPR)*, pp. 5197–5206, 2015.
- [71] P. Krähenbühl, C. Doersch, J. Donahue, and T. Darrell, “Data-dependent initializations of convolutional neural networks.” arXiv, 2016. [Online]. Available: <https://arxiv.org/abs/1511.06856>
- [72] D. Pathak, R. Girshick, P. Dollár, T. Darrell, and B. Hariharan, “Learning features by watching objects move,” in *Proceedings of the IEEE Conference on Computer Vision and Pattern Recognition (CVPR)*, July 2017.
- [73] R. Zhang, P. Isola, and A. A. Efros, “Split-brain autoencoders: Unsupervised learning by cross-channel prediction,” in *Proceedings of the IEEE Conference on Computer Vision and Pattern Recognition*, 2017, pp. 1058–1067.
- [74] M. Noroozi and P. Favaro, “Unsupervised learning of visual representations by solving jigsaw puzzles,” in *European conference on computer vision*. Springer, 2016, pp. 69–84.
- [75] J. Donahue, P. Krähenbühl, and T. Darrell, “Adversarial feature learning.” arXiv, 2016. [Online]. Available: <https://arxiv.org/abs/1605.09782>
- [76] T.-Y. Lin, M. Maire, S. J. Belongie, J. Hays, P. Perona, D. Ramanan, P. Dollár, and C. L. Zitnick, “Microsoft COCO: common objects in context,” in *ECCV*, 2014.
- [77] V. Bychkovsky, S. Paris, E. Chan, and F. Durand, “Learning photographic global tonal adjustment with a database of input/output image pairs,” in *CVPR 2011*. IEEE, 2011, pp. 97–104.
- [78] D.-T. Dang-Nguyen, C. Pasquini, V. Conotter, and G. Boato, “Raise: A raw images dataset for digital image forensics,” in *Proceedings of the 6th ACM multimedia systems conference*, 2015, pp. 219–224.
- [79] E. Agustsson and R. Timofte, “NTIRE 2017 challenge on single image super-resolution: Dataset and study,” in *2017 IEEE Conference on Computer Vision and Pattern Recognition Workshops (CVPRW)*, 2017, pp. 1122–1131.
- [80] D. Scharstein, R. Szeliski, and R. Zabih, “A taxonomy and evaluation of dense two-frame stereo correspondence algorithms,” in *Proceedings IEEE Workshop on Stereo and Multi-Baseline Vision (SMBV 2001)*, 2001, pp. 131–140.
- [81] S. Su, M. Delbracio, J. Wang, G. Sapiro, W. Heidrich, and O. Wang, “Deep video deblurring for hand-held cameras,” in *2017 IEEE Conference on Computer Vision and Pattern Recognition (CVPR)*, 2017, pp. 237–246.
- [82] J. Yosinski, J. Clune, Y. Bengio, and H. Lipson, “How transferable are features in deep neural networks?” *Advances in neural information processing systems*, vol. 27, 2014.

APPENDIX

A. Overview of the Supplementary Material

A lot of data was gathered and aggregated for this work, too much to fit in the paper. Instead, this data is made available as supplementary material. The supplementary material is available in three different versions: An online spreadsheet², three ancillary .csv files published alongside this work, and this appendix.

Each version of the supplementary material serves a different purpose. The online spreadsheet contains the raw attributes and performance metrics as well as the derived attributes, aggregated results, and automatic generation of scatterplots similar to those found in this work. This facilitates quick access to and analysis of the data for the readers. The ancillary files contain the same raw data and derived attributes as the spreadsheet and are meant to guarantee that the raw data is available even if the online spreadsheet at some point becomes unavailable. The appendix contains the raw performance metrics of the four experiments so that they may be easily accessible while reading.

The performance metrics for the different architectures and extraction points for each of the four experiments are available in the following tables: Table VII (Experiment 1), Table VIII (Experiment 2), Tables IX–XII (Experiment 3), and Table XIII (Experiment 4).

TABLE VII

TEST ACCURACY ON SVHN AND STL-10 FOR DOWNSTREAM MODELS USING AUTOENCODER ENCODINGS TRAINED WITH DIFFERENT LOSS NETWORKS

Architecture	SVHN				STL-10			
	E	S	M	L	E	S	M	L
<i>VGG Networks</i>								
VGG-11	0.826	0.832	0.860	0.825	0.381	0.453	0.567	0.724
VGG-16	0.826	0.833	0.887	0.837	0.413	0.512	0.592	0.741
VGG-16_bn	0.816	0.820	0.863	0.492	0.434	0.318	0.247	0.465
VGG-19	0.826	0.833	0.896	0.821	0.397	0.499	0.607	0.736
<i>Residual Networks</i>								
ResNet-18	0.820	0.832	0.867	0.471	0.422	0.473	0.415	0.465
ResNet-50	0.821	0.833	0.862	0.571	0.413	0.554	0.413	0.480
ResNeXt-50 32x4d	0.819	0.830	0.864	0.259	0.419	0.383	0.428	0.403
<i>Inception Networks</i>								
GoogLeNet	0.814	0.868	0.849	0.595	0.373	0.474	0.540	0.593
InceptionNet v3	0.803	0.846	0.828	0.366	0.301	0.475	0.528	0.354
<i>EfficientNet</i>								
EfficientNet_B0	0.818	0.828	0.838	0.714	0.393	0.384	0.434	0.695
EfficientNet_B7	0.807	0.821	0.851	0.445	0.418	0.277	0.648	0.385
<i>Uncategorized Networks</i>								
AlexNet	0.818	0.817	0.799	0.744	0.387	0.596	0.640	0.669
DenseNet-121	0.758	0.831	0.862	0.264	0.442	0.488	0.565	0.578
SqueezeNet	0.825	0.845	0.843	0.791	0.405	0.513	0.639	0.681

²bit.ly/loss-network-analysis

TABLE VIII
CORRECTNESS, COMPLETENESS, AND QUALITY ON THE MRD TESTSET FOR U-NET MODELS TRAINED WITH DIFFERENT LOSS NETWORKS

Architecture	Correctness				Completeness				Quality			
	E	S	M	L	E	S	M	L	E	S	M	L
<i>VGG Networks</i>												
VGG-11	31.0	28.6	22.9	41.7	45.4	42.5	34.7	64.0	17.6	16.3	13.0	23.7
VGG-16	41.3	31.5	38.2	34.7	63.5	45.9	57.4	50.2	23.5	17.9	21.7	19.7
VGG-16_bn	32.3	36.1	34.9	29.8	47.1	54.6	53.2	43.9	18.4	20.5	19.9	17.0
VGG-19	39.2	37.8	42.1	29.0	60.9	56.9	64.4	43.0	22.4	21.5	23.9	16.5
<i>Residual Networks</i>												
ResNet-18	27.7	33.0	35.7	26.5	41.3	48.1	54.2	39.7	15.8	18.8	20.3	15.1
ResNet-50	40.1	22.5	26.9	30.6	62.0	34.2	40.2	44.8	22.8	12.8	15.3	17.4
ResNeXt-50 32x4d	36.5	23.3	40.5	33.5	55.1	35.3	62.4	48.6	20.7	13.3	23.1	19.0
<i>Inception Networks</i>												
GoogLeNet	25.3	24.1	26.1	36.9	38.2	36.6	39.1	55.7	14.4	13.8	14.9	21.0
InceptionNet v3	25.7	24.9	38.6	40.9	38.7	37.5	57.8	62.9	14.7	14.2	21.9	23.3
<i>EfficientNet</i>												
EfficientNet_B0	33.9	31.9	34.8	35.9	49.2	46.5	48.9	49.8	19.3	18.1	19.5	21.3
EfficientNet_B7	23.7	39.0	41.3	43.4	35.9	58.3	60.9	61.8	13.5	22.2	24.0	25.6
<i>Uncategorized Networks</i>												
AlexNet	27.3	28.1	32.7	37.3	40.7	41.8	47.5	56.3	15.5	16.0	18.6	21.2
DenseNet-121	34.3	34.3	30.2	35.3	49.7	33.7	44.3	53.7	19.5	12.6	17.2	20.1
SqueezeNet	21.6	39.6	29.4	24.5	33.2	61.4	43.4	36.9	12.3	22.6	16.8	13.9

TABLE IX
PSNR OF $\times 4$ UPSCALING ON SET 5, SET 14, AND BSD100 OF AN IMAGE TRANSFORMATION NETWORK TRAINED WITH DIFFERENT LOSS NETWORKS

Architecture	Set 5				Set 14				BSD100			
	E	S	M	L	E	S	M	L	E	S	M	L
<i>VGG Networks</i>												
VGG-11	30.7	28.6	28.1	27.2	26.4	24.9	24.7	24.7	26.3	24.9	24.7	25.2
VGG-16	30.3	27.2	24.9	25.5	26.3	24.7	23.7	24.1	25.9	24.9	23.8	23.9
VGG-16_bn	28.6	28.5	23.2	13.2	24.7	24.5	21.9	14.3	25.2	24.4	22.7	15.4
VGG-19	30.2	26.1	26.2	26.8	26.3	24.1	24.0	24.0	26.1	24.3	24.2	23.5
<i>Residual Networks</i>												
ResNet-18	28.7	26.8	28.3	25.5	25.4	24.1	24.8	23.1	25.9	24.5	24.6	23.6
ResNet-50	29.1	31.0	28.4	24.1	25.5	25.7	25.0	22.5	25.4	25.2	24.8	24.5
ResNeXt-50 32x4d	29.8	27.3	29.5	24.7	25.9	24.7	25.1	22.4	26.0	25.1	25.3	22.7
<i>Inception Networks</i>												
GoogLeNet	26.5	29.5	28.4	26.0	24.2	25.3	24.7	23.5	24.7	25.0	24.9	24.6
InceptionNet v3	27.4	27.4	26.3	24.9	24.2	24.7	24.0	23.7	24.5	25.4	24.0	24.0
<i>EfficientNet</i>												
EfficientNet_B0	21.1	26.8	27.3	25.8	20.7	24.5	24.3	24.1	21.1	25.0	24.8	24.5
EfficientNet_B7	28.6	27.7	27.9	26.1	25.5	24.8	24.6	23.4	25.6	25.8	24.9	23.5
<i>Uncategorized Networks</i>												
AlexNet	29.9	29.2	30.0	29.7	25.7	24.9	25.2	25.2	25.7	25.1	24.9	24.9
DenseNet-121	24.8	30.1	29.3	25.1	23.4	25.2	25.2	22.4	24.0	24.9	24.9	24.5
SqueezeNet	31.1	29.1	28.4	26.9	26.5	25.0	24.8	23.9	26.2	25.3	24.6	24.1

TABLE X

MSSIM OF $\times 4$ UPSCALING ON SET 5, SET 14, AND BSD100 OF AN IMAGE TRANSFORMATION NETWORK TRAINED WITH DIFFERENT LOSS NETWORKS

Architecture	Set 5				Set 14				BSD100			
	E	S	M	L	E	S	M	L	E	S	M	L
<i>VGG Networks</i>												
VGG-11	0.855	0.772	0.812	0.793	0.690	0.603	0.630	0.643	0.646	0.546	0.579	0.602
VGG-16	0.859	0.824	0.806	0.804	0.689	0.649	0.640	0.643	0.639	0.603	0.589	0.583
VGG-16_bn	0.834	0.832	0.807	0.382	0.664	0.660	0.653	0.318	0.613	0.604	0.614	0.357
VGG-19	0.856	0.809	0.815	0.803	0.693	0.641	0.639	0.625	0.641	0.587	0.591	0.551
<i>Residual Networks</i>												
ResNet-18	0.826	0.838	0.834	0.805	0.672	0.665	0.669	0.629	0.638	0.628	0.619	0.574
ResNet-50	0.835	0.856	0.837	0.742	0.671	0.677	0.668	0.619	0.621	0.623	0.617	0.618
ResNeXt-50 32x4d	0.840	0.836	0.846	0.824	0.678	0.671	0.673	0.647	0.636	0.631	0.628	0.594
<i>Inception Networks</i>												
GoogLeNet	0.822	0.847	0.832	0.773	0.655	0.670	0.651	0.615	0.621	0.618	0.598	0.592
InceptionNet v3	0.786	0.825	0.813	0.779	0.615	0.667	0.653	0.627	0.568	0.626	0.609	0.590
<i>EfficientNet</i>												
EfficientNet_B0	0.749	0.815	0.826	0.808	0.617	0.668	0.663	0.649	0.587	0.637	0.622	0.606
EfficientNet_B7	0.826	0.803	0.812	0.797	0.663	0.648	0.648	0.629	0.615	0.616	0.607	0.582
<i>Uncategorized Networks</i>												
AlexNet	0.828	0.803	0.815	0.814	0.665	0.627	0.624	0.632	0.618	0.581	0.562	0.573
DenseNet-121	0.784	0.851	0.845	0.777	0.628	0.678	0.674	0.624	0.592	0.625	0.626	0.604
SqueezeNet	0.861	0.816	0.831	0.808	0.693	0.641	0.655	0.637	0.646	0.596	0.605	0.582

TABLE XI

PSNR OF $\times 8$ UPSCALING ON SET 5, SET 14, AND BSD100 OF AN IMAGE TRANSFORMATION NETWORK TRAINED WITH DIFFERENT LOSS NETWORKS

Architecture	Set 5				Set 14				BSD100			
	E	S	M	L	E	S	M	L	E	S	M	L
<i>VGG Networks</i>												
VGG-11	26.2	26.0	22.8	19.6	22.8	22.5	20.9	18.4	22.6	22.1	21.3	19.0
VGG-16	25.2	23.4	19.9	18.6	22.5	21.4	19.5	19.0	22.3	21.5	20.1	19.7
VGG-16_bn	24.6	21.6	13.2	12.0	21.6	20.0	13.0	11.9	21.3	20.1	13.9	12.8
VGG-19	25.4	22.5	19.7	20.0	22.6	21.0	19.3	19.1	22.5	21.3	20.0	19.4
<i>Residual Networks</i>												
ResNet-18	25.6	24.9	23.2	22.1	22.4	21.8	20.5	20.3	22.3	21.5	20.7	20.9
ResNet-50	24.7	25.3	25.1	23.3	21.9	21.7	21.6	21.0	22.1	21.3	21.3	21.3
ResNeXt-50 32x4d	25.5	25.3	25.0	14.7	22.4	21.9	21.5	15.7	22.3	21.7	21.2	16.2
<i>Inception Networks</i>												
GoogLeNet	22.0	25.7	25.2	24.1	20.9	21.9	21.7	21.3	21.2	21.5	21.5	21.1
InceptionNet v3	22.6	24.2	23.8	24.5	20.7	21.7	21.7	21.9	21.3	21.7	21.7	21.8
<i>EfficientNet</i>												
EfficientNet_B0	18.4	24.4	25.4	24.8	18.8	22.0	22.2	22.0	19.3	22.2	21.9	21.8
EfficientNet_B7	25.0	23.5	25.8	24.6	22.2	21.3	22.4	21.8	22.4	21.9	22.2	22.0
<i>Uncategorized Networks</i>												
AlexNet	26.3	25.8	25.5	24.2	22.6	21.9	21.9	21.4	22.1	21.5	21.6	21.4
DenseNet-121	21.4	24.1	24.9	23.9	20.8	21.6	21.9	21.3	21.4	21.8	21.5	21.4
SqueezeNet	26.5	25.0	23.8	22.1	22.9	22.0	21.5	20.6	22.6	21.7	21.0	20.4

TABLE XII

MSSIM OF $\times 8$ UPSCALING ON SET 5, SET 14, AND BSD100 OF AN IMAGE TRANSFORMATION NETWORK TRAINED WITH DIFFERENT LOSS NETWORKS

Architecture	Set 5				Set 14				BSD100			
	E	S	M	L	E	S	M	L	E	S	M	L
<i>VGG Networks</i>												
VGG-11	0.709	0.675	0.590	0.604	0.487	0.452	0.389	0.413	0.452	0.391	0.354	0.377
VGG-16	0.673	0.666	0.605	0.569	0.463	0.453	0.417	0.420	0.420	0.413	0.390	0.394
VGG-16_bn	0.685	0.649	0.518	0.380	0.478	0.458	0.385	0.282	0.448	0.443	0.401	0.321
VGG-19	0.696	0.661	0.591	0.574	0.481	0.450	0.402	0.399	0.441	0.419	0.373	0.369
<i>Residual Networks</i>												
ResNet-18	0.685	0.657	0.673	0.532	0.480	0.446	0.465	0.374	0.449	0.392	0.424	0.357
ResNet-50	0.678	0.688	0.685	0.588	0.479	0.464	0.456	0.402	0.443	0.416	0.398	0.375
ResNeXt-50 32x4d	0.696	0.695	0.690	0.341	0.483	0.476	0.468	0.272	0.449	0.438	0.413	0.290
<i>Inception Networks</i>												
GoogLeNet	0.617	0.695	0.673	0.620	0.454	0.459	0.460	0.427	0.438	0.414	0.401	0.369
InceptionNet v3	0.634	0.661	0.656	0.628	0.451	0.448	0.462	0.437	0.420	0.400	0.431	0.409
<i>EfficientNet</i>												
EfficientNet_B0	0.592	0.669	0.688	0.667	0.436	0.469	0.466	0.460	0.413	0.443	0.413	0.428
EfficientNet_B7	0.674	0.644	0.662	0.599	0.470	0.447	0.467	0.409	0.442	0.433	0.423	0.382
<i>Uncategorized Networks</i>												
AlexNet	0.681	0.636	0.631	0.611	0.469	0.413	0.412	0.406	0.425	0.366	0.364	0.364
DenseNet-121	0.605	0.648	0.650	0.582	0.438	0.459	0.436	0.398	0.428	0.419	0.388	0.364
SqueezeNet	0.710	0.606	0.627	0.611	0.491	0.406	0.417	0.417	0.455	0.362	0.354	0.369

TABLE XIII

2AFC AND JND SCORES OF THE BAPPS DATASET FOR DIFFERENT LOSS NETWORKS USED TO MEASURE DEEP PERCEPTUAL SIMILARITY

Architecture	2AFC score				JND score			
	E	S	M	L	E	S	M	L
<i>VGG Networks</i>								
VGG-11	0.635	0.650	0.659	0.682	0.545	0.564	0.573	0.623
VGG-16	0.637	0.641	0.653	0.671	0.557	0.552	0.567	0.614
VGG-16_bn	0.629	0.636	0.642	0.669	0.545	0.545	0.556	0.621
VGG-19	0.635	0.639	0.653	0.666	0.557	0.547	0.568	0.608
<i>Residual Networks</i>								
ResNet-18	0.629	0.647	0.654	0.674	0.517	0.545	0.559	0.604
ResNet-50	0.629	0.661	0.658	0.659	0.525	0.561	0.573	0.593
ResNeXt-50 32x4d	0.628	0.639	0.652	0.658	0.526	0.540	0.558	0.589
<i>Inception Networks</i>								
GoogLeNet	0.631	0.677	0.682	0.667	0.512	0.542	0.563	0.567
InceptionNet v3	0.625	0.669	0.659	0.660	0.516	0.572	0.559	0.555
<i>EfficientNet</i>								
EfficientNet_B0	0.626	0.621	0.665	0.651	0.530	0.540	0.598	0.587
EfficientNet_B7	0.629	0.624	0.658	0.638	0.513	0.551	0.579	0.536
<i>Uncategorized Networks</i>								
AlexNet	0.643	0.686	0.691	0.688	0.518	0.569	0.586	0.589
DenseNet-121	0.628	0.648	0.668	0.661	0.506	0.544	0.576	0.579
SqueezeNet	0.635	0.679	0.685	0.678	0.527	0.573	0.602	0.606